Biodegradable binary blends of poly (butylene succinate) or poly (ε-caprolactone) with poly (butylene succinate-*ran*-ε-caprolactone) copolymers: Crystallization behavior

Maryam Safari [1] [*], Ricardo A. Pérez-Camargo [2*], Laura Ballester-Bayarri [1], Guoming Liu [2,3], Agurtzane Mugica[1], Manuela Zubitur [4], Dujin Wang [2,3] and Alejandro J. Müller [1,5] [*]

[1]POLYMAT and Department of Polymers and Advanced Materials: Physics, Chemistry and Technology, Faculty of Chemistry, University of the Basque Country UPV/EHU, Donostia-San Sebastián 20018, Spain.

[2]Beijing National Laboratory for Molecular Sciences, CAS Key Laboratory of Engineering Plastics, Institute of Chemistry, Chinese Academy of Sciences, Beijing 100190, China

[3]University of Chinese Academy of Sciences, Beijing 100049, China

[4] POLYMAT and Department of Polymers and Advanced Materials: Physics, Chemistry and Technology, Faculty of Chemistry, University of the Basque Country UPV/EHU, Donostia-San Sebastián 20018, Spain.

[5] IKERBASQUE, Basque Foundation for Science, Plaza Euskadi 5, Bilbao 48009, Spain

*Corresponding author: maryam.safari@polymat.eu, ricardo507@iccas.ac.cn, alejandrojesus.muller@ehu.es.
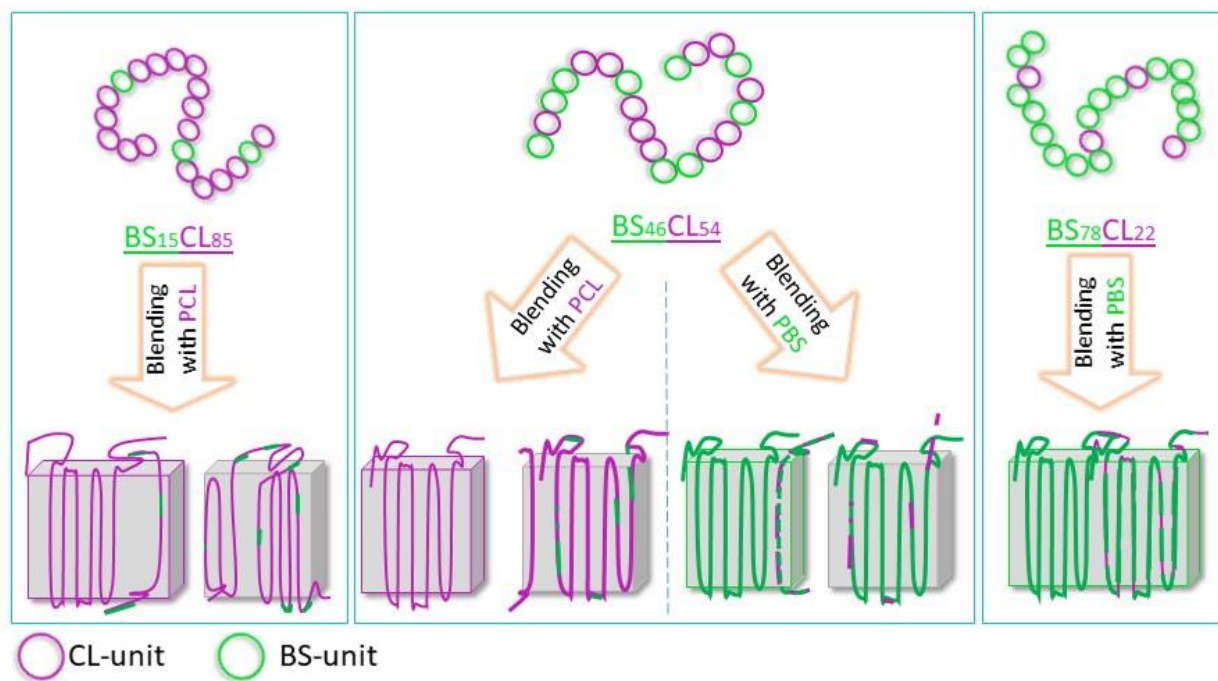
Graphical Abstract

ABSTRACT

Poly (butylene succinate) (PBS) and polycaprolactone (PCL) are two immiscible biocompatible and biodegradable polymers. Aiming to combine the properties of these biodegradable polymers, this work explores for the first time blending PBS or PCL with PBS-*ran*-PCL copolymers (BS_xCL_y) at 75/25, 50/50, and 25/75 wt% compositions, with various copolymer contents: $BS_{78}CL_{22}$, $BS_{46}CL_{54}$, and $BS_{15}CL_{85}$. The crystallization behavior of these novel binary blends was systematically studied with non-isothermal and isothermal differential scanning calorimetry (DSC), polarized light optical microscopy (PLOM), and simultaneous wide- and small-angle X-ray scattering (WAXS and SAXS). All the blends displayed a miscible character in the amorphous state, judging by a single glass transition temperature, and in the melt state (as indicated by SAXS), but their miscibility in the crystalline state depends on the specific blend. In both $PBS/BS_{78}CL_{22}$ and $PCL/BS_{15}CL_{85}$ evidences of co-crystallization between the matrix and the crystallizable fraction of the copolymer were found. However, high comonomer exclusion, higher in the $BS_{15}CL_{85}$ than in the $BS_{78}CL_{22}$, greatly affects blend miscibility. Thus, the results show that the $PBS/BS_{78}CL_{22}$ blend is miscible, in the crystalline state, at high PBS (homopolymer) content, i.e., 75/25 and 50/50 compositions, whereas its "counterpart", the $PCL/BS_{15}CL_{85}$ displays partial miscibility, even for high PCL (homopolymer) content. For the 25/75 blends, i.e., copolymer-rich, the homopolymer addition favors the crystallization of the copolymer-rich component. Blending PBS or PCL with $BS_{46}CL_{54}$ leads to blends that exhibit a much lower miscibility in the crystalline state than the blends prepared with BS or CL-rich copolymers, independently of the composition. But, interestingly, a novel behavior is found, since the $BS_{46}CL_{54}$ copolymer can crystallize either in PBS type crystals or in PCL type crystals depending on the polymeric matrix (PCL or PBS). The PBS favors the crystallization of the BS component, while the PCL favors the crystallization of the CL component within the random copolymer. The crystallization behavior found in this work evidences the interactions of the PBS or PCL with the BS_xCL_y copolymer, representing a potential strategy to combine the properties of the PBS and PCL through blending.

1. INTRODUCTION

Nowadays, there is a significant concern regarding excessive plastic waste generation [1], mainly for single-use non-biodegradable plastics, which creates substantial environmental pollution and other related problems. On the one hand, some solutions for this problem require measurements to improve the waste management policies or legislation to limit the non-biodegradable plastics for particular applications [2]. On the other hand, a complementary emerging solution uses biodegradable polymers as an alternative since they can degrade and form water, carbon dioxide, and biomass [3-4].

Biodegradable polymers have drawbacks in their mechanical properties, processability, and prices, making it difficult to compete with well-known commodities, e.g., polyolefins. The most straightforward strategy to overcome these drawbacks is polymer blending. Polymer blending, an efficient and economical technique, offers the possibility of combining the parent components' physicochemical, mechanical, and degradation properties (due to the interactions among the components [5]) [6-9]. In some cases, the immiscible character of the parent components affects the properties due to the phase separation. Therefore, compatibilizers and other strategies might overcome this problem, leading to improved properties.

Poly (butylene succinate) (PBS) and poly (ε-caprolactone) (PCL) are biocompatible and biodegradable semicrystalline polyesters with a balance of properties that can be

4

exploited in several applications. PCL possesses good ductility and elasticity due to its low glass transition temperature, T_g, and it is easy to process by different processing techniques. In addition, the raw materials for PCL preparation are cost-effective and accessible [10]. However, its use in some applications is limited by low mechanical strength [11] and low deformation temperature (melting point ~ 60 °C). As reflected in many recent reviews [12-14] PBS is a promising material, with a relatively high melting point crucial for some applications. It is easy to process (compared to other aliphatic polyesters), is compatible with conventional polymer processing techniques [14], and its loading capacity and physical properties resemble polyethylene (PE) and polypropylene (PP). This latter feature is attractive because PE and PP are often used for short-shelf time products like packaging and mulch films [14]. Nevertheless, PBS's high crystallinity implies a low degradation rate and barrier properties. The combination of PBS and PCL properties through blending might offer interesting physical and biodegradation properties, in which the PCL with a high degradation rate shows better tensile strength, while PBS with a much slower degradation rate shows better toughness. Thus, PBS/PCL blending might allow exploiting the combined properties of the PBS and PCL in several applications, e.g., biomedical and packaging [15-16].

PBS/PCL blends have been much studied [17-24]. Independently of the preparation method (melt vs. solution blending), the PBS/PCL blends are thermodynamically immiscible, leading to macro-phase separation and poor interfacial adhesion [17]. This is evidenced by composition-independent T_g, and a phase-separated melt. Despite the immiscibility of the PBS/PCL blends, interesting characteristics have been reported. In a recent review, Gumede et al. [17] reported that the increase of the PCL content in the blend

5

provoked an increase in the elongation at break and impact strength but a decrease in the tensile strength. Nugroho et al. [18] reported improved processability for 70/30 PBS/PCL blends subjected to γ rays action between 10 and 50 kGy, enhancing the melt strength. Huang et al. [10] found that PBS/PCL blends degraded even faster than the PCL in a soil culture solution. Higher biodegradation of PBS/PCL membranes in compost compared to neat PCL was found by Sadeghi et al. [25] These authors prepared PBS/PCL membranes with PBS content of 10, 20, and 30 %, and found the highest biodegradation with 20 % of PBS content, due to the augmented membrane porosity and hydrophilicity provoked by PBS addition.

In addition to the homopolymer/homopolymer blends, blending homopolymers with copolymers also offers the possibility of combining the properties of both components. This is an interesting blending strategy because, on the one hand, the copolymer might have interesting properties, e.g., higher degradation rates, and, on the other hand, one of the components of the copolymer might provide the desired interactions with the homopolymer matrix to enhance the miscibility of the blend components. The homopolymers/copolymers blends can have different aims, such as tuning the microdomain morphology of block copolymers [26-27], studying particular crystallization and segregation [28] behaviors, and of course, tailoring specific properties. An example of the latter is the poly (lactic acid), PLA, blended with PLA-*ran*-glycolic acid copolymers, PGA, PLA-*ran*-PGA. This blend aims to tailor the degradation rate by combining a rapid degrading component, PLA-*ran*-PGA, with a slower degrading one, PLA [29]. In this case, the presence of the PLA in the copolymers helps in the miscibility of the blend. Similarly, blending PBS or PCL with its random copolymers, PBS-*ran*-PCL (BS_xCL_y), seems an interesting but unexplored strategy to

6

combine the properties of the PBS with the CL-component of the copolymer, or PCL with the BS-component of the copolymer, with enhanced miscibility due to the presence of a BS- or CL-components in the copolymer, respectively. As far as the authors know, the blends of PBS or PCL with its BS_xCL_y copolymers have not been investigated yet.

This study explores for the first time the crystallization behavior, due to its close relationship with the mechanical and degradation properties, of PBS/BS_xCL_y and PCL/BS_xCL_y blends. These novel binary blends were prepared, by solution blending, in different compositions (75/25, 50/50, and 25/75 compositions) and varying the BS_xCL_y content: $BS_{78}CL_{22}$, $BS_{46}CL_{54}$, and $BS_{15}CL_{85}$. They were thermally (non-isothermal and isothermal differential scanning calorimetry (DSC)), morphologically (polarized light optical microscopy (PLOM)), and structurally (simultaneous wide- and small-angle X-ray scattering (WAXS/SAXS)) characterized. The analysis, including the Nishi-Wang approach and T_g vs. composition, of the different experimental data, evidence a miscible character for the PBS/$BS_{78}CL_{22}$ blend and much-reduced miscibility for the PCL/$BS_{15}CL_{85}$. An interesting and novel behavior was found for the PBS/$BS_{46}CL_{54}$ and PCL/$BS_{46}CL_{54}$ binary blends. The $BS_{46}CL_{54}$ crystallization depends on the matrix (forming PCL type crystals when blended with PCL or exclusive PBS type crystals when blended with PBS). Nonetheless, the PBS/$BS_{46}CL_{54}$ are partially miscible, and the PCL/$BS_{46}CL_{54}$ exhibit much-reduced miscibility. Overall, the results show a wide range of properties depending on blend components and blend ratio, allowing the possibility to tailor the properties of these novel biodegradable blends for specific applications.

2. EXPERIMENTAL

2.1. Materials

PBS was supplied by Nature-Plast under the trade name PBE003 with a number average molecular weight, M_n, of 19800 g/mol [30]. The PCL was supplied by Ravago Chemicals under the trade name Capa-6250, with an average molecular weight in weight, M_w, of 25000 g/mol [31]. 1,4-butanediol (BD), ε-caprolactone (CL), dimethyl succinate (DMS), and titanium tetraisopropoxide (TTP) (as the catalyst) were purchased from Aldrich and were used as received.

PBS-*ran*-PCL copolymers, here named BS_xCL_y, have been synthesized and characterized in our recent work [32] through two polycondensation stages and melt reaction. The transesterification and the ring-opening reaction of dimethyl succinate (DMS), 1,4-butanediol (BD), and ε-caprolactone (CL) were performed, obtaining high molecular weight BS_xCL_y copolymers. The composition of the copolymers was determined by nuclear magnetic resonance, H^1 NMR, and the M_w and M_n by GPC using poly (methyl methacrylate), PMMA, standard and HFIP solvent. The main characteristics of the neat homopolymers and copolymers used in this work are listed in Table 1.

Table 1. Results (M_n, M_w, and Dispersity ($Đ$)) of the synthesis of the copolymerization of BS and CL.

Copolyester	M_n (g/mol)	M_w (g/mol)	$Đ$
PBS	19800	79250	4.0
$BS_{78}CL_{22}$	19750	51400	2.6

$BS_{46}CL_{54}$	26000	60700	2.3
$BS_{15}CL_{85}$	26350	53100	2.0
PCL	N.A.	25000	N.A.

2.2. Preparation of the Binary blends.

The binary blends were prepared in solution, using chloroform as the solvent. Around 20 mg of the sample were dissolved in 2 mL of chloroform, and then the solution was introduced into glass vials. Next, they were shaken and allowed to evaporate under the hood. After a few hours, the chloroform level was reduced, and the vials were placed in the vacuum-oven at 40 ºC for 1 day. In Table 2, the prepared blend samples with different ratios are listed.

Table 2. Prepared binary blends and their compositions.

$PBS/BS_{78}CL_{22}$	$PBS/BS_{46}CL_{54}$
$PBS/BS_{78}CL_{22}$ (25/75)	$PBS/BS_{46}CL_{54}$ (25/75)
$PBS/BS_{78}CL_{22}$ (50/50)	$PBS/BS_{46}CL_{54}$ (50/50)
$PBS/BS_{78}CL_{22}$ (75/25)	$PBS/BS_{46}CL_{54}$ (75/25)
$PCL/ BS_{46}CL_{54}$	$PCL/BS_{15}CL_{85}$
$PCL/BS_{46}CL_{54}$ (25/75)	$PCL/BS_{15}CL_{85}$ (25/75)
$PCL/BS_{46}CL_{54}$ (50/50)	$PCL/BS_{15}CL_{85}$ (50/50)
$PCL/BS_{46}CL_{54}$ (75/25)	$PCL/BS_{15}CL_{85}$ (75/25)

2.3. Characterization techniques

2.3.1. Differential Scanning Calorimetry (DSC)

DSC measurements were performed using a PerkinElmer (8000-Pyris model) calorimeter equipped with a cooling system (Intracooler 2P), under nitrogen atmosphere flow, 20 mL/min, and calibrated with indium (T_m = 156.61 °C and ΔH_m = 28.71 J/g). The samples were weighed ($\sim$ 5 mg) and sealed in standard aluminum pans.

Non-isothermal measurements were performed according to the following steps: (1) Heating the as received sample from 25 °C to T (i.e., the temperature to erase the thermal history = 30 °C above the melting temperature), registering the first heating scan; (2) Erasing the previous thermal history by heating the samples to T for 3 min; (3) Cooling (recording the cooling scan) the molten sample to $-$ 60 °C at a controlled rate (20 °C/min); (4) Holding the sample at $-$ 60 °C for 1 minute; (5) Heating up (recording the second heating scan) from $-$ 60 °C to T at a controlled rate (20 °C/min).

Isothermal measurements were performed using the procedures recommended by Lorenzo et al. [33] and recently reviewed by Pérez-Camargo et al. [34]. These authors suggested a thermal protocol to determine the minimum isothermal crystallization temperature, $T_{c,\ min}$. The $T_{c,\ min}$ guarantees that the material does not crystallize when it is cooled from the melt to $T_c \geq T_{c,\ min}$ before the isothermal step. Thus, the isothermal crystallization from the melt is carried out by selecting $T_c \geq T_{c,\ min}$. The isothermal crystallization procedure is represented in Scheme S1, and described in the following lines:

10

(1) Erasing the thermal history at T for 3 minutes; (2) Cooling down to the chosen crystallization temperature, $T_c \geq T_{c, min}$, at a controlled cooling rate of 60 ºC/min; (3) Isothermal step at the chosen T_c for a sufficient time to complete crystallization, e.g., three times the half-crystallization peak; (4) Heating from T_c to T at a rate of 10 °C/min. Note that the melting temperature, T_m, of the crystals crystallized at specified T_c can be obtained from this heating. This is the set of data, T_m vs. T_c, required to determine the equilibrium melting temperature, $T_m°$, with the Hoffman-Week (HW) extrapolation [35-36]. The T_m vs. T_c plot for obtaining the extrapolated $T_m°$ values of PBS and PCL is plotted in Figure S1 (Section S2 on the SI).

2.3.2. Polarized Light Optical Microscopy (PLOM)

In this study, a BX-51 model Olympus optical microscope was used, equipped with a digital camera (Olympus SC-50) and a Linkam (TP-91 model) hot-stage. The samples, i.e., neat PBS and PCL and their binary blends with copolymers (PBS/BS$_x$CL$_y$, PCL/BS$_x$CL$_y$), were sandwiched in between cover glasses, forming thin films. The growth rate of spherulites, G, as a function of T_c was determined through PLOM, using the isothermal DSC protocol described above. In this case, a cooling rate of 50 °C/min was selected (the maximum controlled cooling rate allowed by the Linkam equipment).

Throughout the different temperatures, the growth of the spherulites was recorded, taking about ten images per isothermal crystallization temperature, and then the radius of the spherulites was measured using the OLYMPUS Stream software. Once the radius (r) had

been obtained, it was plotted as a function of time (t). This data has a linear relationship (see Equation 1) which is linearly fitted.

$$r = Gt \qquad \text{Eq. 1}$$

The slope obtained corresponds to the growth rate of the spherulite, G, which is plotted against the different crystallization temperatures.

2.2.3. Simultaneous in situ Wide-Angle and Small-Angle X-ray Scattering (WAXS/SAXS)

Selected samples were examined under non-isothermal conditions by simultaneous in situ WAXS/SAXS performed at beamline BL11-NCD at the ALBA Synchrotron radiation facility in Barcelona, Spain. The energy of the X-ray source was 12.4 keV ($\lambda = 1.0$ Å). The beamline BL11-NCD provided a WAXS detector, Rayonix LX255-HS, with an active area of 230.4×76.8 mm (pixel size: 44 μm^2), and a SAXS detector, Pilatus 1M (from Dectris)), with an activated image area of 168.7×179.4 mm^2, a total number of pixels of 981×1043, and a pixel size of 172×172 μm^2. For the WAXS configuration, a sample–detector distance of 15.5 mm with a tilt angle of 27.3° was used, and for SAXS, the distance was 6463 mm. The measurements were taken simultaneously with a frame rate of 25 frames per second. The intensity profile was output as the plot of the scattering intensity vs. scattering vector, $q = 4\pi$ $\sin (\theta)\lambda^{-1}$, where λ is the X-ray wavelength ($\lambda = 1$ Å) and 2θ is the scattering angle. The scattering vector was calibrated using silver behenate (SAXS) and chromium (III) oxide (WAXS).

The samples in DSC pans were placed in a Linkam hot stage (THMS-600 model) coupled to a liquid nitrogen cooling system. The thermal protocols applied in the DSC experiments were reproduced in the Linkam hot stage, i.e., first heating, cooling, and second heating scans at 20 °C/min, recording SAXS/WAXS spectra every 6 seconds.

3. RESULTS AND DISCUSSION

The combination of the PBS and PCL properties might be helpful for specific applications; however, blending both components leads to an immiscible blend. The immiscibility of PBS/PCL blends has been widely reported in the literature [17, 37]. To take advantage of the PBS and PCL properties, despite their immiscibility, here we explore, for the first time, blending BS_xCL_y copolymers, with a variable composition, with PBS or PCL matrices. Are these novel binary (PBS/BS_xCL_y or PCL/BS_xCL_y) blends immiscible? How are these blends affected by the BS_xCL_y composition? This section will answer these questions, by studying the crystallization behavior, and hence the miscibility, of PBS/BS_xCL_y (Section 3.1.1) and PCL/BS_xCL_y binary blends (Section 3.1.2).

3.1. Evaluating thermal transitions with non-isothermal DSC experiments.

Different thermal transitions, such as glass transition, crystallization, cold-crystallization, and melting temperatures (T_g, T_c, T_{cc}, T_m) and their related enthalpies (ΔH_m, ΔH_c, ΔH_{cc}), were obtained from cooling and second heating DSC scans. The crystallinity, X_c, of the different blends was estimated using the measured enthalpies, and the equilibrium melting enthalpies, $\Delta H_m°$ determined by the group contribution semi-empirical theory of Van Krevelen [38]: 110.3 and 139.5 J/g for PBS and PCL. The obtained value for the PCL is in

13

line with the literature [39], whereas a higher value has been recently reported for PBS [40]. All the thermal transitions, enthalpies, and X_c values are listed in Tables S1 to S5.

The T_g vs. blend composition study is accepted as a precise and reliable method to assess polymer miscibility in blends when the difference between the T_g values of the parent components of the blend is larger than 10 °C [41]. In T_g vs. blend composition data, obtained by DSC, a single T_g between the parent components indicates the miscibility or homogeneity of the blend components on a scale of about 10 nm. Even with this miscibility criteria, detailed analysis could also consider the broadening (or fluctuations) of the T_g width, ΔT_g, with composition (see Tables S1 to S5). The ΔT_g broadening might indicate borderline miscibility or more complex phenomena, such as heterogeneity on a segmental level or fluctuations of the local concentrations, or other fluctuations as proposed in the self-concentration model [42-43]. Here, we adopted a simple analysis. Despite the lowest T_g differences being ~ 4 °C and the highest ~ 24 °C, we have assumed that a single T_g for the whole blend's compositions represents one piece of evidence to assess polymer miscibility or homogeneity. A deeper understanding of the T_g evolution escapes from the scope of this work.

In this work, a single T_g value is obtained for all the blends, independently of the composition, revealing their miscibility in the amorphous state. In some cases, some deviation from a simple mixing rule was obtained. Recently, Huang et al. [44] studied the molecular origin of the T_g deviations from a linear relationship in copolymers. One factor that provokes T_g deviations is related to the affinity or repulsion interactions of the

components, which has also been reported in blends [45]. The affinity interactions, like hydrogen bonding, lead to a negative enthalpy of mixing, ΔH_{mix}, and positive deviations from the simple mixing rule. The opposite situation is found in repulsion interactions: positive ΔH_{mix} and negative deviation.

During the crystallization from the melt, in the crystalline state, miscible and partially miscible behaviors can be elucidated (together with other morphological and structural evidences (shown below)) judging by the positions and areas of the melting transitions of the blend. For clarity, the discussion is divided into PBS/BS$_x$CL$_y$ (Section 3.1.1) and PCL/BS$_x$CL$_y$ (Section 3.1.2) binary blends. The study of the BS$_x$CL$_y$ random copolymers is presented in Section S4 (Figure S2) on the SI, revealing an isodimorphic behavior, in line with our previous works [46-49]. Isodimorphism is a crystallization mode in random copolymers. Considering an isodimorphic PA-*ran*-PB copolymer, the inclusion of B co-units within PA type crystals and vice-versa allows the crystallization of the copolymer in the entire composition range. The isodimorphic copolymers display a pseudo-eutectic behavior in their properties (see Figure S2a), typically T_m, as a function of the comonomer content. Structurally, at one side of the pseudo-eutectic point, the copolymer crystallizes with PA type crystals with some inclusion of B co-units, provoking slight distortions in the unit cell of PA, and the opposite is recorded on the other side of the pseudo-eutectic point (see Figure S2b). At the pseudo-eutectic point, both PA and PB type crystals with the inclusion of B and A co-units have the chance to crystallize, and then both structures can coexist [46-49].

15

3.1.1. Binary blends: PBS matrix (PBS/BS_xCL_y random copolymers)

Figure 1 shows the cooling and second heating scans for the PBS/BS$_{78}$CL$_{22}$ (Figures 1a and b) and PBS/BS$_{46}$CL$_{54}$ (Figures 1c and d) binary blends at different compositions (25/75, 50/50, and 75/25). We adopted the following terminology: PBS or PCL for homopolymer transitions and BS$_{fraction}$ or CL$_{fraction}$ for copolymers transitions. The assignment of the different transitions is based on the large differences between homopolymer and copolymer transitions, and the evidence of the characterization techniques discussed in the next sections.

The blends of PBS with the BS$_{78}$CL$_{22}$ copolymer show single exothermic and endothermic peaks (see Figures 1a and b), indicating they are most probably miscible in the crystalline state, i.e., the BS$_{fraction}$ in the copolymer co-crystallizes (crystallization of both components in the same lamellar crystals) with PBS. The BS$_{fraction}$ is covalently bonded with CL units, and vice-versa, and hence here it is considered as a different phase than the PBS or PCL homopolymer, despite the chemical similarities. It should be noted that the CL$_{fraction}$ within the BS$_{78}$CL$_{22}$ copolymer does not crystallize (see ref. [46] to our previous works) as it is a minority fraction. In contrast, blends with the BS$_{46}$CL$_{54}$ copolymer (in the pseudo-eutectic position) lead to partially miscible (see Figures 1c and d) systems because there are separated but shifted exothermic and endothermic peaks for each component.
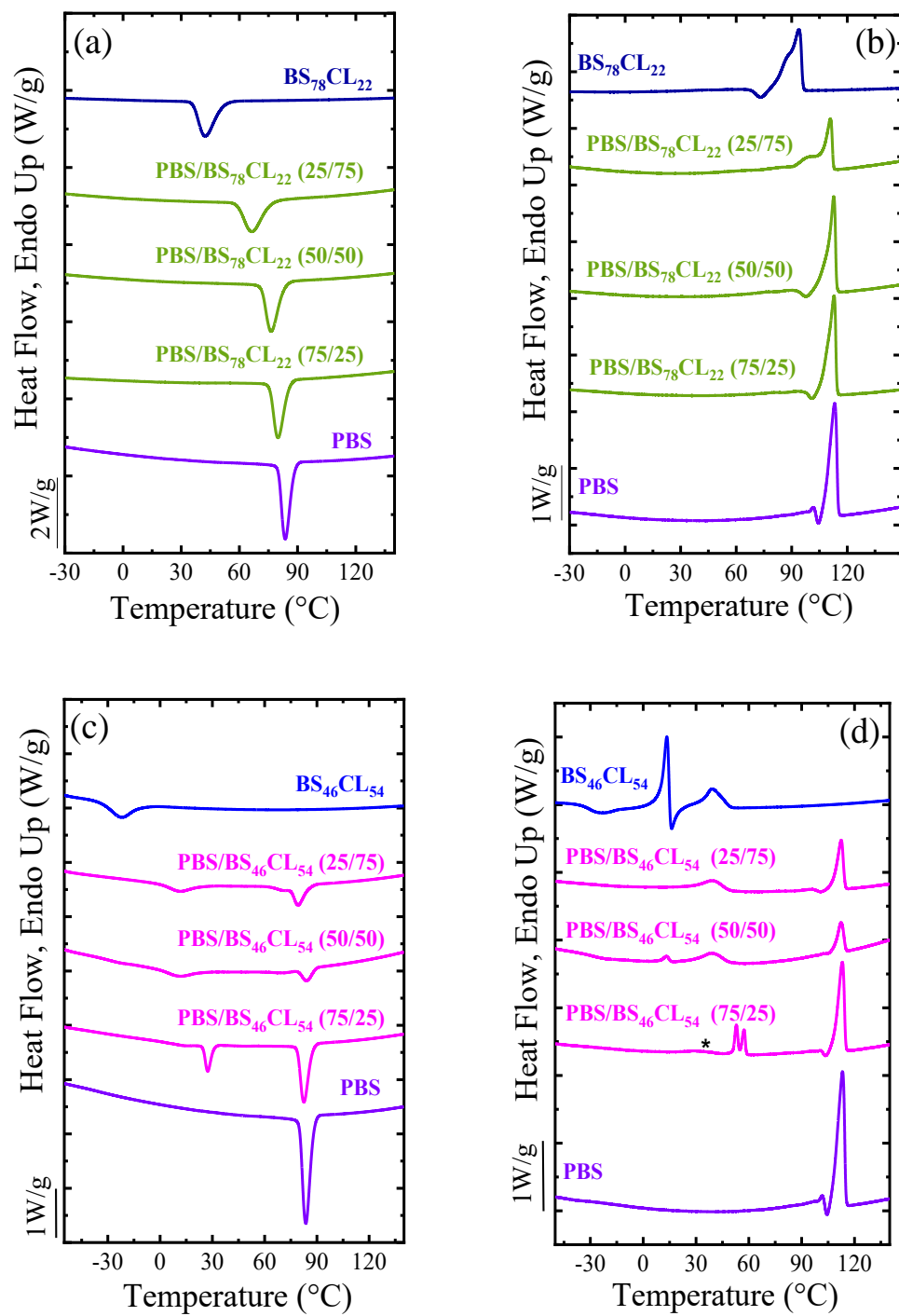
16

Figure 1. DSC cooling (a,c) and second heating (b,d) scans, at 10 °C/min, for PBS/BS$_{78}$CL$_{22}$ (a,b) and PBS/BS$_{48}$CL$_{54}$ (c,d) blends. The asterisk indicates a small endothermic signal.

For the PBS/BS$_{78}$CL$_{22}$ blends (Figures 1a and b), there is a single T_g value (see Section S4, Figure S2c) at all compositions, which practically follows a simple mixing law, in the T_g vs. PBS content curve (see Figure 2a), suggesting the miscibility, of the amorphous phase, of the blend (no phase segregation occurs). Likewise, there is a single T_c.

The analysis of the heating scans (Figure 1b) reveals a single T_m for the PBS-rich blend compositions (75/25 and 50/50), displaying the typical heating behavior of the neat PBS, exhibiting its characteristic exothermic peak before melting, generally regarded as a recrystallization process during the heating scan [50-51]. Only for the copolymer-rich blend (25/75) a shoulder that might be related to the separate melting of the BS$_{fraction}$ (of the copolymer) is detected, suggesting a partial phase separation. However, in general, the predominant BS$_{fraction}$ favors the miscibility of the copolymer and the PBS matrix.

The PBS/BS$_{46}$CL$_{54}$ blends (see Figures 1c and d) exhibit partial miscibility, depending on the composition. The T_g vs. PBS content curve (see Figure 2a), displaying a single T_g value per composition, positively deviates from a simple mixing rule, a fact that indicates a change in the intermolecular interactions (affinity interactions) within the amorphous regions [44-45]. Moreover, multiple T_c (Figure 1c) and T_m (Figure 1d) values corresponding to the different components (PBS, BS$_{fraction}$, and CL$_{fraction}$) of the blend are registered. The higher CL content, in the BS$_{46}$CL$_{54}$ copolymer, explains this behavior. Nevertheless, the minority BS$_{fraction}$ seems to dominate the crystallization of the copolymer, leading, in most cases, to the BS$_{fraction}$ crystallization, due to the miscibility between the PBS

18

and the BS component. Still, the higher exclusion of CL co-units within the copolymer might significantly affect the PBS-BS$_{fraction}$ interactions.

The BS$_{46}$CL$_{54}$ copolymer has a composition at the pseudo-eutectic point of BS$_x$CL$_y$ copolymers, in which both BS and CL fractions can crystallize. Such crystallization depends on the crystallization conditions, i.e., rate-dependent behavior. Safari et al. [46] reported that low cooling rates, i.e., 1 °C/min, favored the crystallization of the BS$_{fraction}$ since there is enough time to fully grow well-developed spherulites of BS$_{fraction}$, hindering the crystallization of the CL$_{fraction}$. As the cooling rate increases to values of 5 and 10 °C/min, both CL$_{fraction}$ and BS$_{fraction}$ can crystallize, whereas fast cooling rates, e.g., 20 °C/min causes the crystallization of only the CL$_{fraction}$. Similar rate-dependent behavior is reported by Pérez-Camargo et al. in PBS-*ran*-poly (butylene adipate), BS$_x$BA$_y$, copolymers [52]. In this work, a novel behavior is found, since the lowest T_c (see Figure 1c) corresponds to the BS$_{fraction}$ instead of the CL$_{fraction}$, evidencing that the employed cooling rate and the PBS matrix favored the crystallization of the BS$_{fraction}$ during the cooling instead of the crystallization of both CL$_{fraction}$ and BS$_{fraction}$. Nevertheless, as we described below, the CL$_{fraction}$ can cold-crystallize in the subsequent DSC heating scan, as reflected by the appearance of the CL$_{fraction}$ endothermic signals (see Figure 1d).

Figure 1c shows two T_c values during the cooling scan for all the compositions: the BS$_{fraction}$ of the BS$_{46}$CL$_{54}$ copolymer crystallizes at low T_c, whereas the PBS crystallizes at high T_c. Interestingly, when the blend is rich in PBS, the T_c of the BS$_{fraction}$ within the

copolymer is shifted to higher temperatures and becomes sharper. The shift of T_c values may be related to either changes in nucleation or in blend miscibility.

The heating scan (see Figure 1d) shows at least two T_m values: the $BS_{fraction}$ melts at low T_m, and the PBS melts at high T_m. The T_m values for PBS and $BS_{fraction}$ remain practically unchanged for the 25/75 and 50/50 compositions, but they change in the 75/25 composition An extra signal at the lowest temperatures, corresponding to the $CL_{fraction,}$ is detected for the 75/25 and 50/50 compositions. The $CL_{fraction}$, in this case, might crystallize during cooling, as coincident crystallization, or during the heating, cold-crystallization. The thermal behavior of the 75/25 PBS/$BS_{46}CL_{54}$ is peculiar: on the one hand, the $CL_{fraction}$ endotherm becomes broad and shifts to higher values, on the other hand, the $BS_{fraction}$ signal is shifted to higher temperatures but becomes sharp. The $BS_{fraction}$ exothermic peak is sharper for this composition. These observations might indicate that most BS co-units exhibited a higher affinity for the PBS than the CL ones, enhancing their crystallization. Even though the CL co-units seem to show enhanced nucleation (cold-crystallization) because of the PBS, they also are confined by the PBS, explaining the decrease in its melting enthalpy. Similar behavior is registered in PBS/PCL blends [53].

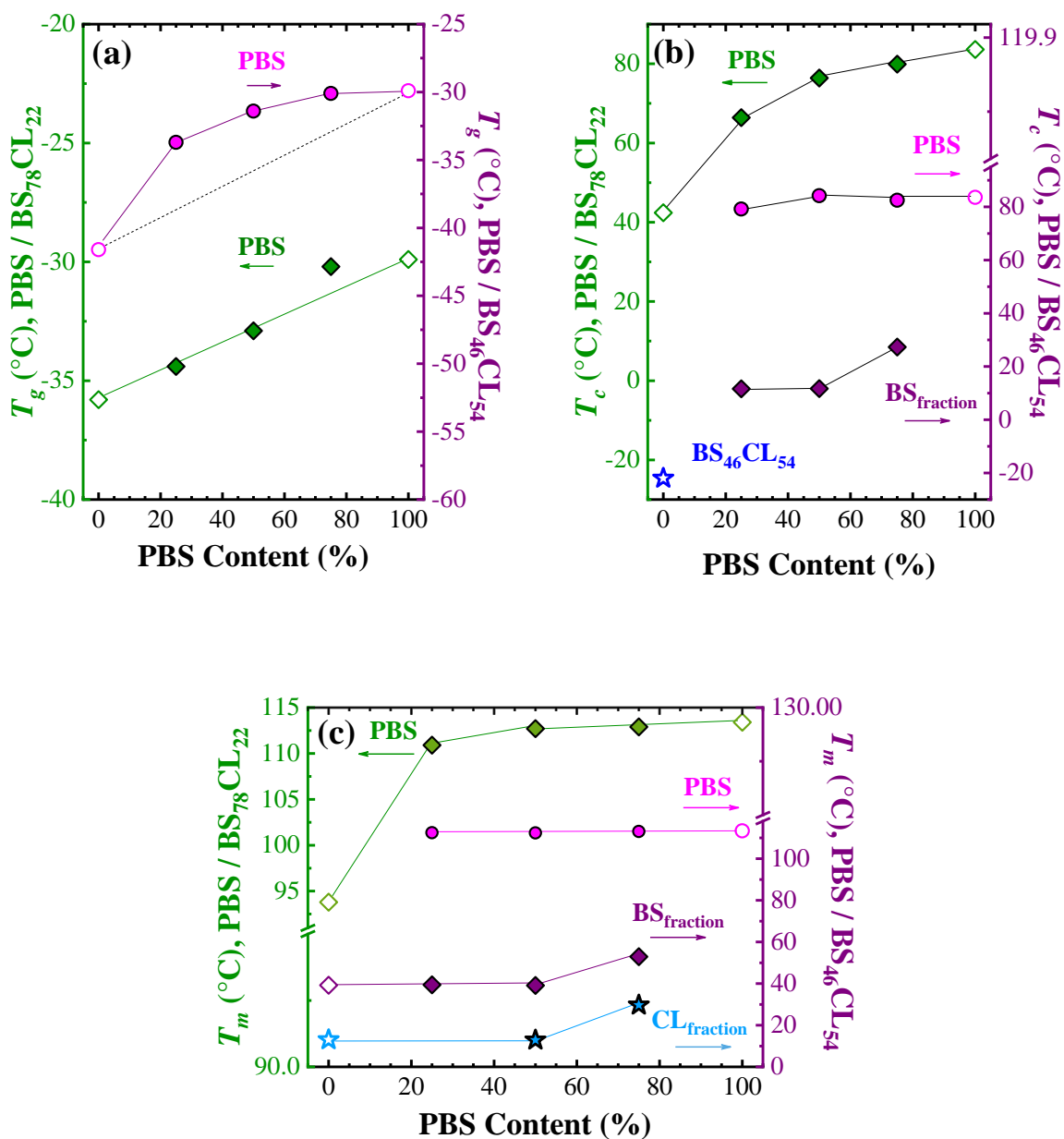**Figure 2.** (a) T_g, (b) T_c, and (c) T_m values as a function of the PBS content. The thermal transitions values are plotted with a double-y-axis: left-y-axis for PBS/BS$_{78}$CL$_{22}$ and right-y-axis for PBS/BS$_{46}$CL$_{54}$ blends.

Figure 2 summarizes the T_g, T_c, and T_m evolution as a function of the PBS content in the blend. The PBS/BS$_{78}$CL$_{22}$ blends are miscible, judging by the displayed single thermal transitions related to PBS (i.e., co-crystallization of PBS and BS$_{fraction}$). Compared with neat PBS, these transitions decrease as the PBS content decreases, indicating the interactions with the copolymer.

The T_g positively deviates from a simple mixing rule in the PBS/BS$_{46}$CL$_{54}$ blend, indicating a change in the nature of the intermolecular interactions (affinity interactions) in the amorphous regions of the blends [44-45]. This change in the intermolecular interactions could have triggered the partial miscibility observed in the crystalline state, as evidenced by the multiple T_c and T_m registered, indicating crystalline phase segregation. The highest copolymer content, and hence the highest CL$_{fraction}$, leads to higher phase segregation, caused by the immiscibility of PBS with the PCL$_{fraction}$. However, at high PBS content, the PBS influences the BS and CL fractions of the BS$_{46}$CL$_{54}$ copolymer, increasing their T_c and T_m. This might be related to a plasticization-like effect and a nucleating effect of the PBS on the copolymer.

3.1.2. Binary blends: PCL matrix (PCL/BS$_x$CL$_y$ random copolymers)

Figure 3 shows multiple exothermic and endothermic peaks, indicating a phase separation process, in the crystalline state, in all the cases (i.e., PCL blended with either BS$_{15}$CL$_{85}$ or BS$_{46}$CL$_{54}$), even when PCL is the majority component in the blend.

Figures 3a and b show the cooling and heating DSC curves for the PCL/BS$_{15}$CL$_{85}$ blend. The BS$_{fraction}$ in BS$_{15}$CL$_{85}$ does not crystallize, as it is a minority fraction within the

22

copolymer (see ref. [32]). Despite the high $CL_{fraction}$ in the copolymer, the blend is only partially miscible in the PCL matrix; this might be related to the higher amount of excluded BS co-units from $CL_{fraction}$ crystals compared with its counterpart, $BS_{78}CL_{22}$ copolymer, limiting the co-crystallization extension.

All the compositions display two exothermic peaks (Figure 3a). At high PCL content, the sharp peak, at high T_c (at 30 ºC), corresponds to the PCL, and the small shoulder, at low T_c (at 14 ºC), to the $CL_{fraction}$. As the PCL content decreases, the T_c of the PCL is slightly shifted to lower values, and the enthalpy becomes lower. The opposite occurs for the T_c and enthalpy of the $CL_{fraction}$, as evidenced by the 25/75 blend (see in Figure 3a the sharp exothermic peak, at low T_c (at 5 ºC), which corresponds to the $CL_{fraction}$).

All the PCL/$BS_{15}CL_{85}$ compositions exhibited two endothermic peaks in the heating scans (see Figure 3b). The lowest T_m (at 30 ºC) is assigned to the $CL_{fraction}$, followed by the melting of PCL at a higher T_m (at 56 ºC), indicating a phase-separation-like behavior. A significant reduction of the $CL_{fraction}$ endothermic peaks areas suggests partial miscibility (as well as the shifts in T_m values with composition) instead of an immiscible behavior. The partially miscible behavior suggests that the $CL_{fraction}$ – PCL interactions are affected by the small $BS_{fraction}$ in the copolymer, e.g., reducing the $CL_{fraction}$ – PCL co-crystallization extension.
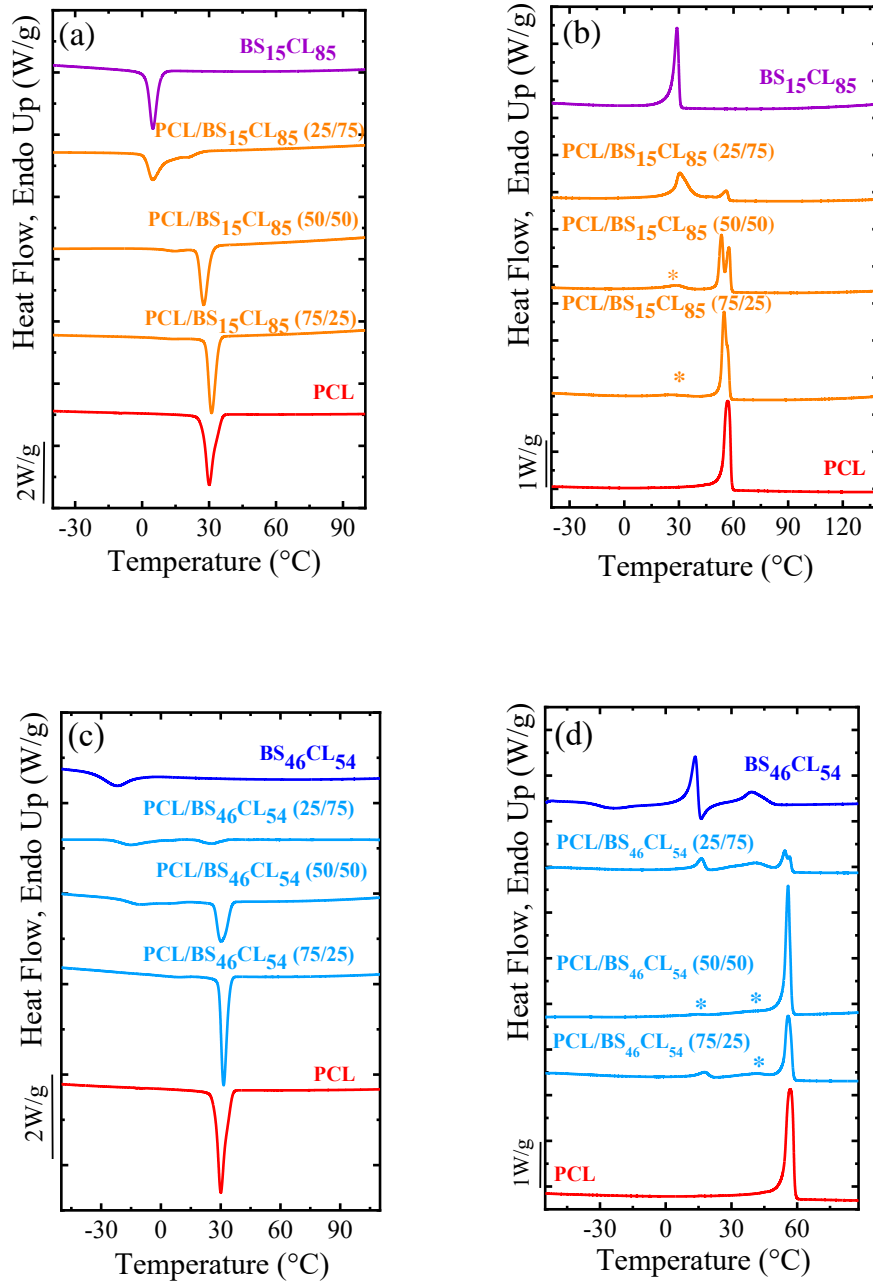
Figure 3. Cooling (a,c) and second heating (b,d) DSC scans for (a,b) PCL/BS$_{15}$CL$_{85}$ and (c,d) PCL/BS$_{46}$CL$_{54}$ blends. All the scans were performed 10 ºC/min. The asterisks indicate the less visible peaks, e.g., for BS$_{fraction}$ in 75/25 and both BS and CL$_{fractions}$ in 50/50 blends.

For the PCL/$BS_{46}CL_{54}$ blend (see Figures 3c and d), the increase of the $BS_{fraction}$, and thus increases the BS co-units exclusion in the copolymer, favors the phase separation in the binary blend, generating a partially miscible blend. Thus, two T_c and multiple T_m (even those corresponding to the $BS_{fraction}$) are observable in Figures 3c and 3d. Figure 3c shows two T_c values for all the compositions. The highest T_c corresponds to the PCL, and it is shifted to lower values as the PCL content decreases. On the other hand, the lowest T_c is assigned to the $CL_{fraction}$, which displays a shift to higher values with increases in PCL content. Recalling the PBS/$BS_{46}CL_{54}$ results, it is interesting to note that the crystallization of the CL or BS fractions of the $BS_{46}CL_{54}$ depends on the matrix. The PBS induces the crystallization of the $BS_{fraction}$, and the PCL the crystallization of the $CL_{fraction}$. This novel effect is similar to the rate-dependent behavior or the crystallization conditions influence found by Safari et al. [46] in the $BS_{46}CL_{54}$ copolymer and Pérez-Camargo et al. [54] in $BS_{40}BA_{60}$ copolymer.

Figure 3d shows the heating curves for all the blends. They exhibited three T_m of different enthalpies depending on the composition. The highest T_m, *circa* 60 °C, corresponds to the PCL, the peak or shoulder at intermediate T_m, *circa* 40 °C, corresponds to the $BS_{fraction}$, and the lowest T_m, *circa* 16 °C, to the $CL_{fraction}$. The $BS_{fraction}$ crystallizes during the heating, i.e., cold-crystallization, although the melting of the $CL_{fraction}$ might overlap the signal of this process. The $BS_{fraction}$ crystallization is not detected during cooling in Figure 3c. Albeit, a coincident crystallization might also be present, as in the 10/90 PBS/PCL binary blends studied by Fenni et al. [19]. The evolution of the different T_g, T_c, and T_m values as a function of the PCL content is plotted in Figure 4.
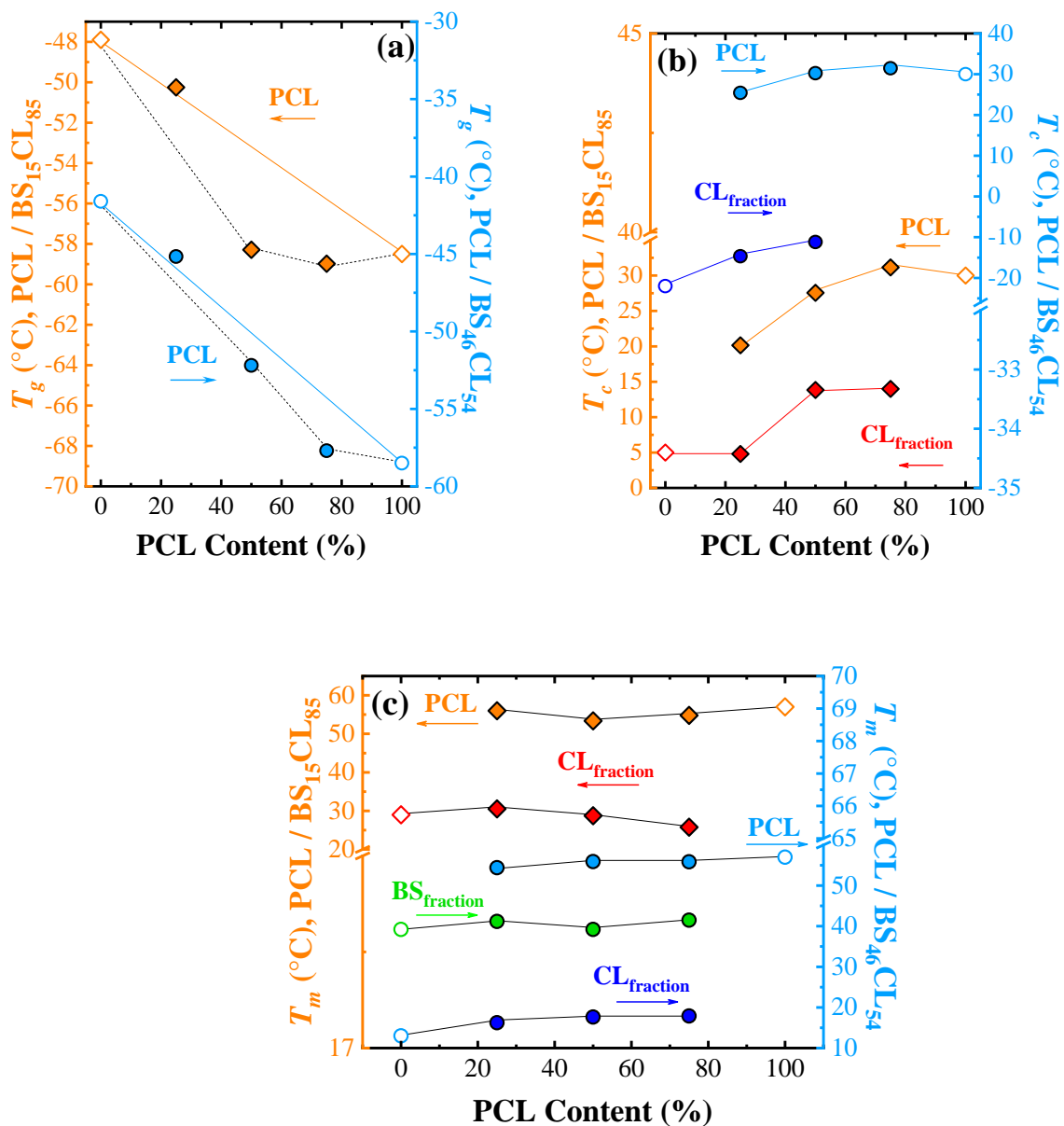
Figure 4. (a) T_g, (b) T_c and (c) T_m values as a function of PCL content. The thermal transitions values are plotted with a double-y-axis: left-y-axis for PCL/BS$_{15}$CL$_{85}$ and right-y-axis for PCL/BS$_{46}$CL$_{54}$ blends.

Figure 4 shows the T_g, T_c, and T_m values as a function of the content of PCL in the blend. The single T_g values of the PCL-based blends, indicates its miscible character in the amorphous state. However, they display a negative deviation of a simple mixing rule. Such negative deviation is often attributed to weak specific interactions [55] and recently to repulsion interactions [44-45]. The found trend explains the different miscibility behavior compared with the PBS-based blends. In the crystalline state, the phase separation of the PCL and the BS and CL fractions of the BS_xCL_y copolymer are clear. The lowest T_c and T_m correspond to the $CL_{fraction}$, and the highest for the PCL. The PCL T_c values decrease due to the copolymer presence, indicating specific interactions. Such a decrease is more significant for the $PCL/BS_{15}CL_{85}$ than the $PCL/BS_{46}CL_{54}$ blend, meaning higher miscibility for the former, as the copolymer contains a higher amount of $CL_{fraction}$. For both blends, the PCL addition favors the crystallization of the $CL_{fraction}$ of the copolymers, as reflected in the shift to higher temperatures of T_m as the PCL content increases. In the case of the $PCL/BS_{46}CL_{54}$ blend, an intermediate T_m of the $BS_{fraction}$ was found, corroborating the phase separation. Despite the phase separation, the T_c and T_m shifts, in both homopolymer and copolymer phases indicating favorable interactions. Nonetheless, more significant displacements of the T_c and T_m were obtained in the PBS/BS_xCL_y blends. This behavior reflects that the PBS–$BS_{fraction}$ interactions are not substantially affected by the $CL_{fraction}$ presence, unlike the PCL–$CL_{fraction}$ interactions, which are clearly affected even by a small amount of $BS_{fraction}$ within the copolymer.

3.2. Isothermal Study

The binary blends studied here could be miscible or partially miscible, as evidenced by the non-isothermal DSC experiments. Interestingly, the copolymer behaves differently depending on the polymeric matrix. Spherulite growth rate (Figure S3 in Section S5) and overall crystallization kinetics are analyzed to understand such behavior further. It is worth noting that the PLOM observations evidenced a homogeneous melt (see Figure S4), while crystallized material shows a homogenous impinged spherulitic morphology, excluding the possibility of macroscopic phase separation.

Figures 5, 6, and 7 show the inverse of the crystallization half-time ($1/\tau_{50\%}$) vs. T_c (isothermal crystallization temperature) for the homopolymers, copolymers, and their binary blends. Figure 5a shows that the PBS crystallizes at higher T_c than the PCL as reported in previous works [48], whereas the $BS_{78}CL_{22}$ and $BS_{15}CL_{85}$ crystallize between the PCL and PBS. The $BS_{46}CL_{54}$, where the $CL_{fraction}$ isothermal crystallization was determined, crystallizes at the lowest T_c values, even lower than neat PCL. In Figure 5b, the T_c (at a constant $1/\tau_{50\%}$) vs. PBS content is plotted, displaying a pseudo-eutectic behavior, typical of isodimorphic random copolymers, with the $BS_{46}CL_{54}$ at the pseudo-eutectic point in line with our previous work [48]. The Lauritzen and Hoffman (LH) theory [56], which can fit both growth rate data (original derivation) and overall crystallization rate (extended application, see Reference [34] for more details), has been employed to fit all the curves (see Figures 5 to 7), using the $T_m°$ values, determined with the HW extrapolation [35] (see Section S2 (Figure S1) on the SI). In this work, the LH theory is only employed for a few comparisons

(see text below), but the analysis of the parameters derived from the theory escaped from the scope of this work; hence, they are not shown.
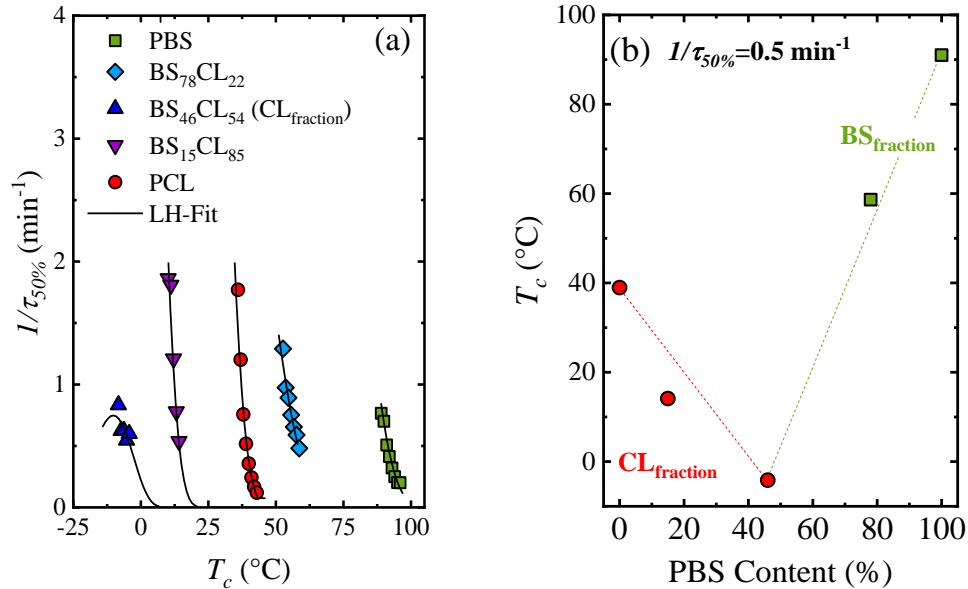

Figure 5. (a) Overall crystallization rates ($1/\tau_{50\%}$) vs. T_c for main components of the binary blends, and (b) T_c vs PBS content measured at a constant $1/\tau_{50\%} = 0.5$ min^{-1}. The solid lines in (a) correspond to the Lauritzen and Hoffman (LH) fit [56] extended to $1/\tau_{50\%}$ vs. T_c data (more details in Reference [34]).

Figure 6 shows the overall isothermal crystallization rate of the PBS/BS$_x$CL$_y$ binary blends. For the PBS/BS$_{78}$CL$_{22}$ blend (see Figure 6a), all the compositions exhibited $1/\tau_{50\%}$ vs. T_c curves in between the parent components, i.e., slower (BS$_{78}$CL$_{22}$) vs. faster (neat PBS) overall crystallization kinetics, as expected. Interestingly, for the blends, as the BS$_{78}$CL$_{22}$ content increases, the $1/\tau_{50\%}$ vs. T_c curves are shifted to higher T_c values, indicating an

acceleration of the crystallization kinetics. When the extreme 75/25 and 25/75 PBS/BS$_{78}$CL$_{22}$ blends are compared, it is clear that the 75/25 composition crystallizes faster. These results align with the faster spherulitic growth kinetics found in the G vs. T_c curves (see Figure S3a), evidencing an interestingly plasticization-like effect of the BS$_{78}$CL$_{22}$ copolymer in the PBS crystallization.

The PBS/BS$_{46}$CL$_{54}$ is partially miscible; hence the crystallization kinetics of both PBS and BS$_{fraction}$ can be followed in this blend, thanks to the significant difference in the T_c range in which they crystallized, see Figures 6b and c. Even though the PBS crystallizes first ($T_c > 85$ °C), the BS$_{fraction}$ signal can be detected at lower isothermal temperatures, e.g., $T_c \sim$ 25 °C. Figures 6b and c show the $1/\tau_{50\%}$ vs. T_c data for the PBS (Figure 6b) and BS$_{fraction}$ (Figure 6c) separately. In the blends rich in PBS (Figure 6b), the copolymer does not cause significant changes in the $1/\tau_{50\%}$ vs. T_c curves (BS$_{fraction}$, Figure 6b), in line with the G vs. T_c curves (see Figure S2b), where copolymer addition does not significantly affect the growth kinetics of the PBS, evidencing the reduced miscibility of this blend.

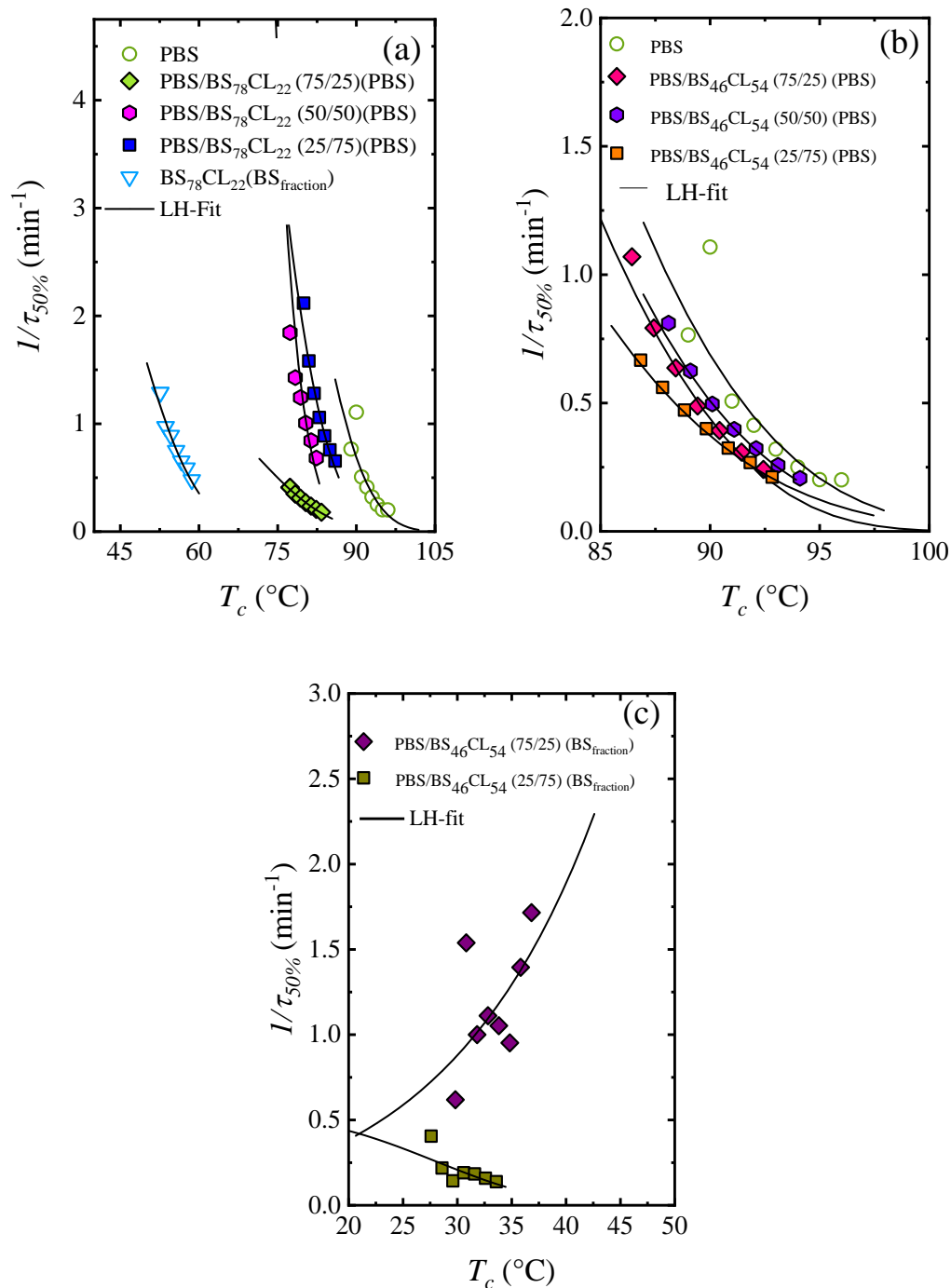**Figure 6.** Overall crystallization rates ($1/\tau_{50\%}$) vs. T_c for (a) PBS/BS$_{78}$CL$_{22}$, (b) PBS/BS$_{46}$CL$_{54}$ (PBS), and (c) PBS/BS$_{46}$CL$_{54}$ (BS$_{fraction}$). Note that for PBS crystallized during cooling before the isothermal step to detect the BS$_{fraction}$ crystallization kinetics. The solid lines correspond to the LH fit [53] extended to $1/\tau_{50\%}$ vs. T_c data (more details in Reference [34])

31

Remarkably, the $BS_{46}CL_{54}$ copolymer can crystallize in the $BS_{fraction}$ instead of the $CL_{fraction}$ (dominant phase in bulk) when PBS is added, as shown in Figure 6c. Thus, the presence of the PBS inhibited the crystallization of the dominant $CL_{fraction}$ (see Figure 5). This demonstrated that, even at isothermal conditions, the crystallization at the pseudo-eutectic point of the isodimorphic copolymer is influenced not only by the crystallization conditions but also by the presence of other components, representing a novel behavior. Figure 6c shows that the $BS_{fraction}$ crystallizes at significantly higher T_c, i.e., T_c around 25 to 35 °C, than the $CL_{fraction}$ (see Figure 5), with T_c below 0 °C. The obtained data for the $BS_{fraction}$ indicates that as the PBS content is higher in the blend, the crystallization of the $BS_{fraction}$ in the copolymer is facilitated.

Figure 7 shows the $1/\tau_{50\%}$ vs. T_c for the PCL/BS_xCL_y binary blends. The crystallization kinetics of both PCL and $CL_{fraction}$ was followed, as noted in Figure 7. Here, the PBS crystallization is not detected in any of the blends. Thus, as in the non-isothermal test, the PCL in the blend favored the crystallization of the $CL_{fraction}$ in the $BS_{46}CL_{54}$ copolymer, even at isothermal conditions.
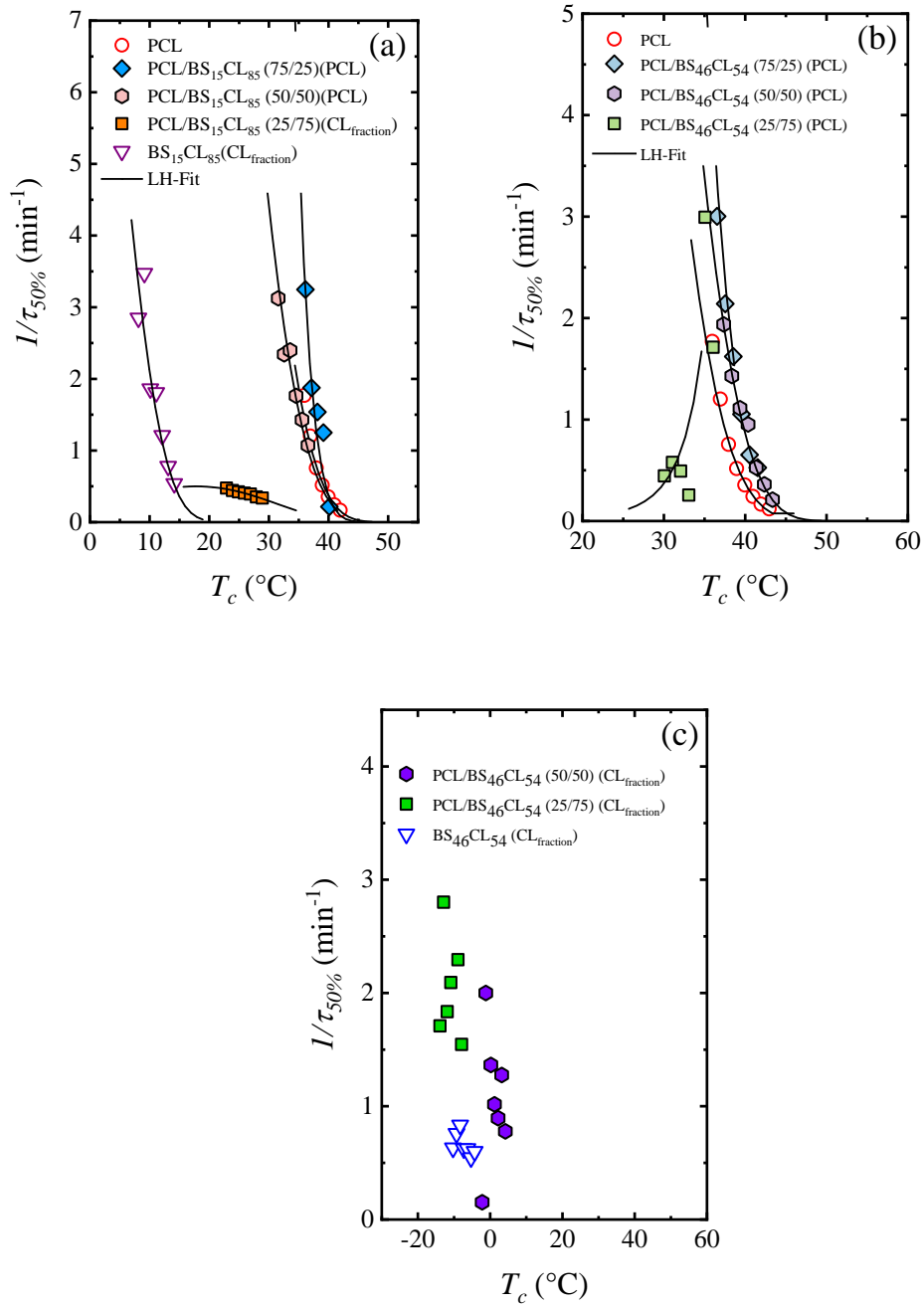
Figure 7. Overall crystallization rates ($1/\tau_{50\%}$) vs. T_c for (a) PCL/BS$_{15}$CL$_{85}$, (b) PCL/BS$_{46}$CL$_{54}$ (PCL), and (c) PCL/BS$_{46}$CL$_{54}$ (CL$_{fraction}$). The solid lines correspond to the LH fit [58] extended to $1/\tau_{50\%}$ vs. T_c data (more details in Reference [34]).

Figure 7a shows that the crystallization kinetics of the blends are in between the parent components (i.e., slower ($BS_{15}CL_{85}$) vs. faster (PCL) crystallization kinetics). In this case, the 75/25 and 50/50 blends have comparable values to the neat PCL, evidencing that copolymer addition does not significantly affect the crystallization kinetics of the PCL. The crystallization kinetics only slows down as the comonomer content increases, i.e., 25 vs. 50 %. These results are in line with the non-isothermal DSC results shown in Figure 4, and, interestingly, are opposite to the effect of the comonomer in the PBS matrix (see Figure 6a). In contrast, the $1/\tau_{50\%}$ vs. T_c data for the 25/75 blend, corresponding to the $CL_{fraction}$ is shifted to higher T_c (compared to the $BS_{15}CL_{85}$ data), indicating an acceleration of crystallization kinetics compared to the $BS_{15}CL_{85}$. Such an effect might be related to a plasticization effect of the PCL on the $CL_{fraction}$ of the copolymer.

Figure 7b show the $1/\tau_{50\%}$ vs. T_c curves of the PCL in the PCL/$BS_{46}CL_{54}$ blend. The $1/\tau_{50\%}$ vs. T_c curves of the 75/25 and 50/50 blends are slightly shifted to the right of the PCL, indicating faster crystallization kinetics. On the contrary, the PCL in the 25/75 blend shows slower crystallization kinetics than neat PCL because the copolymer probably confines the PCL, difficulting its crystallization. In Figure 7c, we have plotted the curves related to the $CL_{fraction}$, which is the fraction that crystallized in the presence of a PCL matrix. In these curves, it can be noticed that the addition of PCL accelerates the crystallization kinetics of the $CL_{fraction}$ in the copolymer. Such behavior might be related to a plasticization effect, which increases as the PCL content increases. However, the high nucleation density prevented us from following the spherulitic growth kinetics of the PCL-based materials.

34

In the isothermal study, we have applied the Avrami theory [57] obtaining Avrami indexes (see Figure S5), n, between 2.5 to 3.5. These range of n values corresponds to spherulites that grow instantaneously or sporadically, depending on the employed T_c. Therefore, the blending process does not affect the spherulitic morphology (also observed in the PLOM measurements) of the different blends.

3.3. Flory-Huggins parameters: Nishi-Wang approach

Further understanding of the blends was obtained by roughly estimating its Flory-Huggins (FH) parameters (χ). With this aim, the T_m depression of a blend is associated with the interactions of its components, and thus, to the miscibility. It is expected that an immiscible blend does not generate a T_m depression, while a miscible blend, especially those with specific interactions between two components, causes a T_m depression. Nishi-Wang [58-59] provides an expression, which can be simplified (see Equation 2), that correlated the melting point depression with the FH parameters.

$$-\frac{\Delta H_v^0 V_1}{RV_2}\left(\frac{1}{T_m^*} - \frac{1}{T_m^0}\right) = \chi_{12}\phi_1^2 \qquad \text{Eq.2}$$

The Nishi-Wang expression was developed for crystalline-amorphous systems. However, considering the large difference of the $T_m°$ in crystalline/crystalline blends, e.g., $T_m°_{PBS} \gg T_m°_{PCL}$, at high temperatures, one of the components can be considered crystalline, and the other acts as an amorphous diluent. Therefore, in Equation 2, subscript 1 identifies

the amorphous phase, and 2 the crystalline one. Φ is the volume fraction, V is the molar volume of repetitive units, ΔH_v° is the melting enthalpy per mole of the repetitive unit, T_m° is the equilibrium melting temperature of the parent component (unblended), and T_m^* is the equilibrium melting temperature of the crystalline polymer in the blend, here taken as T_m for comparison purposes, χ_{12} stands for the FH interaction parameter. The employed parameters and plots related to Equation 2 are presented in Section S7.

All the blends were evaluated with the Nishi-Wang expression. The resulting χ_{12} are listed in Table 3.

Table 3. Polymer–Polymer Interaction Parameter (χ_{12}) Calculated Using the Nishi–Wang Equation (Equation 2).

Blend	χ_{12}
PBS / $BS_{78}CL_{22}$	-0.170
PBS / $BS_{46}CL_{54}$	0.0045
PCL / $BS_{46}CL_{54}$	0.0476
PCL / $BS_{15}CL_{85}$	0.207

The obtained χ_{12} are approximately in line with our experimental results. The PBS/$BS_{78}CL_{22}$ is predicted to be miscible, exhibiting a negative χ_{12}, whereas its PCL analogous blend, the PCL/$BS_{15}CL_{85}$ is predicted to be immiscible with a positive χ_{12} with a value of 0.207. It might be speculated that such a predictive difference is related to the comonomer exclusion/inclusion balance of each BS_xCL_y copolymer. The change in the

composition of the crystalline phase is beyond the scope of Nishi-Wang equation, in which the crystalline phase is pure. For the $BS_{78}CL_{22}$ most of the CL co-units are included in the $BS_{fraction}$ crystals, favoring, or at least not difficulting, the $BS_{fraction} - PBS$ matrix interactions. In contrast, for the $BS_{15}CL_{85}$, the BS co-units are less included, i.e., excluded to the amorphous phase, difficulting the CL – PCL matrix interactions, as well as the co-crystallization extension. The comonomer inclusion/exclusion balance of BS_xCL_y copolymers has been studied in previous works [46-49].

The Nishi-Wang theory predicts positive, but small values of $\chi_{12,}$ which could correspond to partially miscible or miscible blends depending on their specific phase diagram [58]. However, the $BS_{46}CL_{54}$ exhibits higher comonomer exclusion, i.e., the BS and CL fractions have the same chance of crystallizing, significantly affecting the miscibility. In the next section, we explore the structural changes experienced by the blends.

3.4.   Study of binary blends at different compositions by in situ WAXS/SAXS

In situ WAXS/SAXS experiments were performed in the neat PBS, PCL, and PBS or PCL blended with the BS_xCL_y copolymers, with a selected 50/50 composition. The WAXS/SAXS patterns were recorded during the cooling from the melt, and the subsequent heating, performed at a scan rate of 20 °C/min. The WAXS patterns of the PCL (see Figure S7 (c-d)) display main reflections at $q = 15.3$ nm^{-1} and $q = 17.0$ nm^{-1}, and a shoulder a $q = 15.7$ nm^{-1} that can be assigned to (110), (200) and (111) crystal planes, respectively, of the orthorhombic unit cell of the PCL, with $a = 0.748$, $b = 0.498$, and $c = 1.726$ nm [61-62]. For the PBS, the WAXS patterns (see Figure S8 (c-d)) displayed the main reflections at $q = 14.1$

37

nm^{-1} and $q = 16.3$ nm^{-1}, and medium intense reflections at $q = 15.7$ nm^{-1} and $q = 20.3$ nm^{-1} (not shown), assigned to the (020), (110), (021) and (111) crystal planes, respectively, of the monoclinic unit cell of the α-PBS, with $a = 0.532$, $b = 0.9057$, $c = 1.090$ nm, and $\beta = 123.87°$ [63]. The PBS can also crystallize in a β form (monoclinic, with $a = 0.584$, $b = 0.832$, $c = 1.186$ nm, and $\beta = 131.6°$), but only under stretching [64].

According to previous works, the BS$_{78}$CL$_{22}$ and BS$_{15}$CL$_{85}$ WAXS patterns are similar to the PCL and PBS, respectively, with a slight shift in the q positions, due to the comonomer inclusion. The calculated d-spacings are higher than those of the parent components, reflecting changes in the unit cell change, as expected for isodimorphic copolymers [65]. In the case of the BS$_{46}$CL$_{54}$, both comonomers can crystallize sequentially. First, the BS$_{fraction}$ crystallizes at higher temperatures, followed, at lower temperatures, by the CL$_{fraction}$ crystallization. The q positions are also shifted compared to the parent components, registering significant changes in d-spacings.

Figure 8 shows the WAXS and SAXS patterns obtained for PBS/BS$_{78}$CL$_{22}$ (Figure 8a (WAXS) and Figure 8b (SAXS), and PCL/BS$_{15}$CL$_{85}$ (Figure 8c (WAXS) and Figure 8d (SAXS)) blends. The X-ray results for the 50/50 blends using the BS$_{46}$CL$_{54}$ copolymer are shown in Figure 9. All the blends became isotropic when all the crystals were in the melt state. The SAXS patterns in the melt state were compared to assess the melt state's miscibility (see Section S8, Figure S9). It was found that the SAXS signal for PCL-based blends and PBS/BS$_{78}$CL$_{46}$ coincides, suggesting, together with the other evidence (homogeneous melt in the PLOM images and composition-dependent T_m values), the miscibility in the melt state.

Only the PBS/BS$_{46}$CL$_{54}$ exhibited a slight deviation that might indicate partial miscibility instead.

Figure 8a shows that the 50/50 PBS/BS$_{78}$CL$_{22}$ blend displays the same reflections as neat PBS, indicating that PBS dominates the blend crystallization without the interference of the CL$_{fraction}$. The WAXS patterns taken during the subsequent heating (see Figure S10b in Section S8) are in line with the melting of only PBS co-crystals (i.e., PBS co-crystallized with the BS$_{fraction}$). On the other hand, similar reflections are also obtained for the PBS and PBS/BS$_{78}$CL$_{22}$ when the SAXS patterns (see Figure 8b) are evaluated. The calculated long periods (d^*), at -40 °C, see Table S6, are, $d^*_{blend} = 9.34$ nm for the blend and $d^*_{PBS} = 9.15$ nm for neat PBS. The slightly higher d^*_{blend} values suggest the co-crystallization of the PBS and BS$_{fraction}$ (possibly with some CL co-units inclusion in the BS$_{fraction}$), leaving most CL segments in the amorphous inter-lamellar region of the PBS/BS$_{fraction}$ crystals, thus producing a slight increase in d^*_{blend}. Thus, the WAXS and SAXS results indirectly reflect the miscibility of this binary blend in the crystalline state, in line with DSC results.
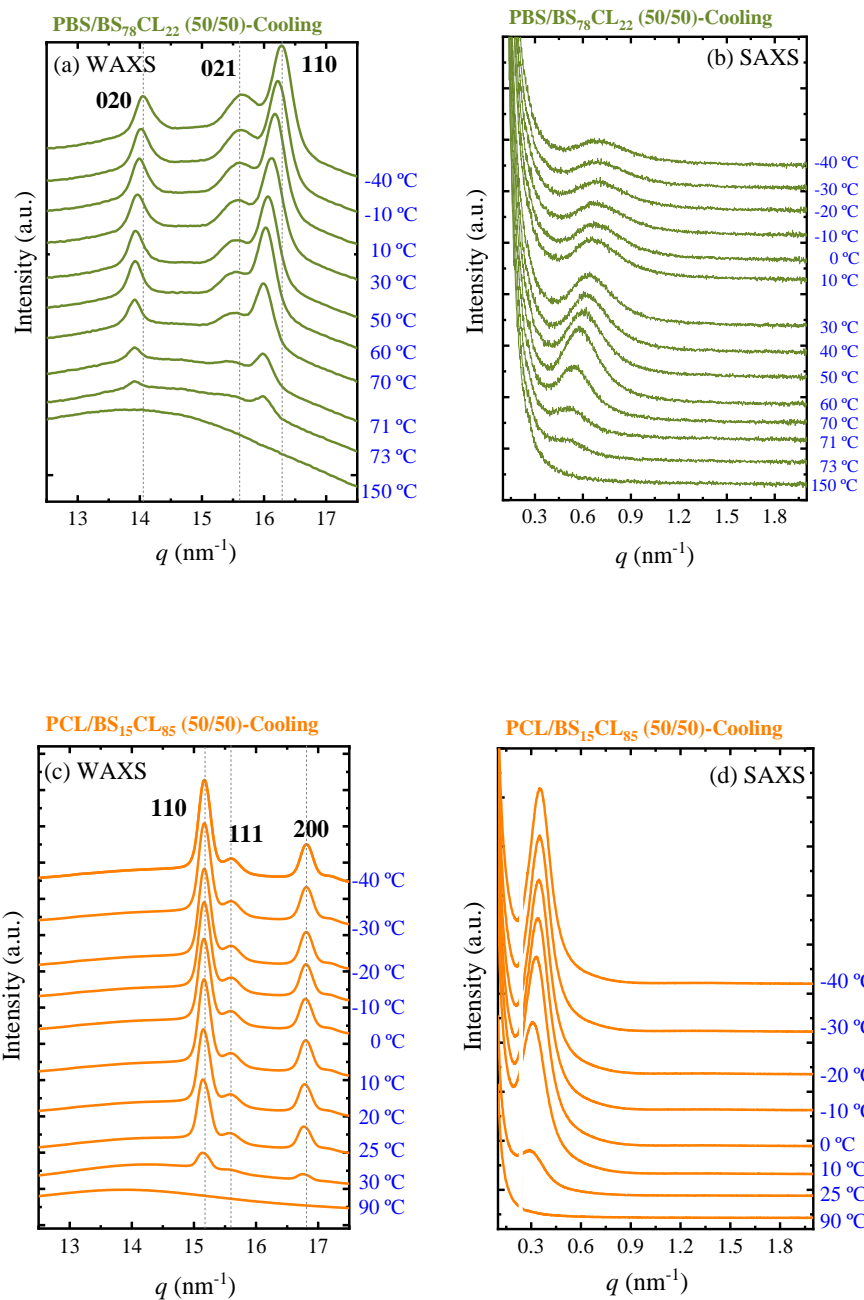
Figure 8. In situ WAXS (a,c) and SAXS (b,d) patterns taken during cooling from the melt, at 20 °C/min for (a,b) PBS/BS$_{78}$CL$_{22}$, and (c,d) PCL/BS$_{15}$CL$_{85}$ binary blends. The main planes of the PBS (Figure 8a) and PCL (Figure 8c) are indicated.

A contrasting behavior is obtained for the 50/50 PCL/BS$_{15}$CL$_{85}$ blend. On the one hand, the BS$_{15}$CL$_{85}$ can distort the crystalline phase of the major PCL phase, as reflected by the higher d-spacing of the blend (slightly lower q values of the blend compared with neat PCL). On the other hand, the long period obtained from the SAXS patterns, at $-$ 40 °C, in Figure 8d, is higher for the blend, $d^*_{blend} = 18.0$ nm vs. $d^*_{PCL} = 12.0$ nm (PCL). In this partially miscible blend, a co-crystallization of the PCL and CL$_{fraction}$ is not discarded. Nonetheless, in this case, the increase of the d^*_{blend} can be produced by a higher BS co-units exclusion. These co-units will be located in the amorphous inter-lamellar regions, producing such an increase in the d^*_{blend}. Summarizing, both WAXS and SAXS results evidence the partially miscible character of this 50/50 PCL/BS$_{15}$CL$_{85}$ blend.

Figure 9 shows the WAXS/SAXS patterns during cooling from the melt of PBS (Figures 9a (WAXS) and 9b (SAXS)) and PCL (Figures 9c (WAXS) and 9d (SAXS)) blended with the BS$_{46}$CL$_{54}$ copolymer. The obtained results demonstrate a remarkable and novel result, i.e., the crystallization of the BS$_{46}$CL$_{54}$ copolymer in its BS crystalline phase in the presence of the PBS matrix and in its CL crystalline phase in the presence of the PCL matrix.

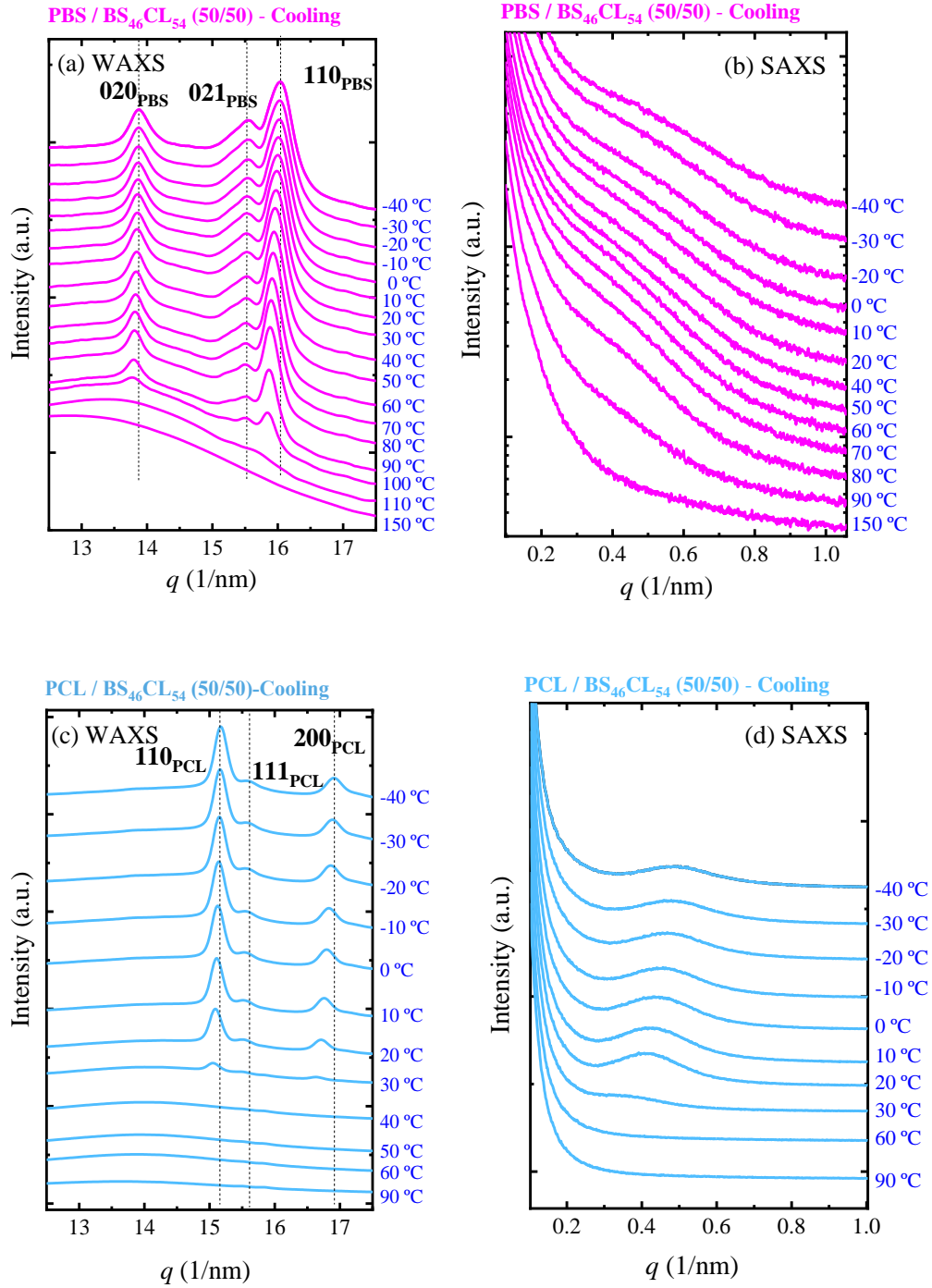**Figure 9.** In situ WAXS (a,c) and SAXS (b,d) patterns taken during cooling from the melt, at 20 °C/min for (a,b) PBS/$BS_{46}CL_{54}$ and (c,d) PCL/$BS_{46}CL_{54}$ binary blends.

For the PBS/BS$_{46}$CL$_{54}$ blend, the WAXS patterns (Figure 9a) resemble those of PBS, even though the BS$_{fraction}$ in the copolymer is in the minority phase. Moreover, no signal corresponding to PCL crystals is obtained. In this case, the main signals are shifted to lower q values; hence, higher d-spacing is generated. This might be related to a distortion of the CL$_{fraction}$ on the PBS unit cell. Similarly, from Figure 9b, the calculated long period of the blend, d^*_{blend} = 12.5 nm, is higher than that of the PBS and the PBS/BS$_{78}$CL$_{22}$ (d^*_{blend} = 9.34 nm); attributed to the partial miscibility provoked by a higher exclusion of CL co-units from the BS$_{fraction}$ crystals.

Figures 9c and 9d, show the WAXS and SAXS patterns for the PCL/BS$_{46}$CL$_{54}$ blends, in which the PCL is the dominant phase, without any traces of PBS crystals reflections. Therefore, the matrix in the blend can hinder the crystallization of the CL$_{fraction}$ or BS$_{fraction}$ in the copolymer, confirming the results obtained with non-isothermal DSC scans. The d^*_{blend} in this case is 12.9 nm, close to the d^*_{PCL} value (12.04 nm), and hence significantly lower than the long period of the PCL/BS$_{15}$CL$_{85}$ blend. This indicates that most of the PCL might crystallize separately from the CL$_{fraction}$, due to the partial miscibility of the blend. Overall, the miscibility with BS$_{46}$CL$_{54}$ is lower than the miscibility that PBS and PCL experience with those copolymers that are rich in either PBS or PCL, i.e., BS$_{78}$CL$_{22}$ and BS$_{15}$CL$_{85}$.

The results indicate a higher affinity of the PBS-based blends with the copolymers than in the PCL-based blends. Still, the changes in thermal transitions and crystallization kinetics indicate a certain degree of interaction in the PCL blends. Thus, PBS or PCL blended

with BS_xCL_y copolymer might represent an interesting strategy to tailor PBS and PCL properties.

4. CONCLUSIONS

This work explored for the first time the crystallization behavior of PBS or PCL blended with PBS-*ran*-PCL copolymers (BS_xCL_y), in different blend ratios, 75/25, 50/50, and 25/75, and by varying the composition within the copolymers: $BS_{78}CL_{22}$, $BS_{46}CL_{54}$, and $BS_{15}CL_{85}$. A systematic characterization of these novel blends was performed through non-isothermal and isothermal DSC studies, PLOM, and simultaneous WAXS/SAXS experiments. All the blends are miscible in the amorphous (single T_g values) and melt state (comparable SAXS signals), and their crystallization is the determining factor for different behaviors in the solid-state. The PBS/$BS_{78}CL_{22}$ blend exhibited only one crystal phase for the PBS-rich (75/25 and 50/50) compositions (miscible), showing thermal transitions and crystallization kinetics between the parent components. Structurally, the *d*-spacing of the studied 50/50 blend is similar to that of neat PBS, while its long period is higher than that of neat PBS, indicating the co-crystallization of the PBS and $BS_{fraction}$, with excluded CL co-units to the amorphous part located in the inter-lamellar region of the PBS/$BS_{fraction}$ crystals. The 25/75 PBS/$BS_{78}CL_{22}$ display a double melting behavior, indicating partial miscibility, generating the slowest crystallization kinetics with respect to the PBS. In contrast, for the PCL/$BS_{15}CL_{85}$ blends, two crystalline phases are found independently of the composition, even when PCL is the major phase. But, the variations in the positions and areas of the transitions indicate a partially miscible behavior. This behavior is also reflected by only slight changes in the crystallization kinetics, followed by both PCL and $CL_{fraction}$. Structurally there are changes in

44

the *d*-spacing, and significantly higher long periods for the blend. This was explained by the co-crystallization of the PCL and $CL_{fraction}$, but, with a high amount of excluded BS co-units to the amorphous part located in the inter-lamellar region.

An interesting and novel behavior was found for both PBS/$BS_{46}CL_{54}$ and PCL/$BS_{46}CL_{54}$ binary blends. It was found that the $BS_{46}CL_{54}$ crystallization depends on the matrix. The $BS_{46}CL_{54}$ copolymer can form exclusive $CL_{fraction}$ crystals when it is blended with PCL or exclusive $BS_{fraction}$ crystals when blended with PBS, even during isothermal experiments. Still, the PBS/$BS_{46}CL_{54}$ are partially miscible, and the PCL/$BS_{46}CL_{54}$ exhibit a much reduced miscibility. For the former, the excluded CL co-units provoke an increase in the long periods, whereas, for the PCL/$BS_{46}CL_{54}$, the excluded BS co-units generated lower long periods than the PCL/$BS_{15}CL_{85}$, indicating a phase-segregation like behavior. In summary, in binary blends, there is a higher affinity of PBS with the $BS_{fraction}$ of the copolymer, including the $BS_{46}CL_{54}$, in comparison with the lower affinity of PCL with the $CL_{fraction}$ of the copolymer, in line with calculated Flory-Huggins parameters, using the Nishi-Wang approach, that indicates a miscible character for the PBS/$BS_{78}CL_{22}$ blend, and a much reduced miscibility for the PCL/$BS_{15}CL_{85}$. It is likely that the higher crystallization ability of the PBS can even affect the CL-rich copolymer. This work demonstrates that miscibility, and thus properties, can be tailored depending on the ratio of the homopolymer/random copolymer blend components.

ACKNOWLEDGMENTS

5. REFERENCES

[1] B.K.H. Lim, E.S. Thian, Biodegradation of polymers in managing plastic waste-A review. Sci. Total. Environ. (2021) 151880, https://doi.org/10.1016/j.scitotenv.2021.151880.

[2] O. Platnieks, S. Gaidukovs, V.K. Thakur, A. Barkane, S. Beluns, Bio-based poly (butylene succinate): Recent progress, challenges and future opportunities. Eur. Polym. J. 161 (2021) 110855, https://doi.org/10.1016/j.eurpolymj.2021.110855.

[3] W. Amass, A. Amass, B. Tighe, A review of biodegradable polymers: uses, current developments in the synthesis and characterization of biodegradable polyesters, blends of biodegradable polymers and recent advances in biodegradation studies. Polym. Int. 47 (1998)

89-144, https://doi.org/10.1002/(SICI)1097-0126(1998100)47:2<89::AID-PI86>3.0.CO;2-F.

[4] J.R. Jambeck, R. Geyer, C. Wilcox, T.R. Siegler, M. Perryman, A. Andrady, R. Narayan, K.L. Law, Plastic waste inputs from land into the ocean. Science 347 (2015) 768–771, https://doi.org/10.1126/science.1260352.

[5] F.P. La Mantia, M. Morreale, L. Botta, M.C. Mistretta, M. Ceraulo, R. Scaffaro, Degradation of polymer blends: A brief review. Polym. Degrad. Stab. 145 (2017) 79-92, https://doi.org/10.1016/j.polymdegradstab.2017.07.011.

[6] D.R. Paul, C.B. Bucknall, Polymer Blends, Vols. 1 and 2., John Wiley & Sons, New York, 2000.

[7] H. Kim, D. Kawaguchi, K. Tanaka, Y. Seo, Fracture Mechanism Change at a Heterogeneous Polymer–Polymer Interface Reinforced with in Situ Graft Copolymers. Langmuir 34 (2018) 11027-11033, https://doi.org/10.1021/acs.langmuir.8b01860.

[8] E. Manias, L.A. Utracki, Thermodynamics of Polymer Blends, Polymer Blends Handbook Springer, The Netherlands, 2014.

[9] M.J. Folkes, P.S. Hope, Polymer blends and alloys, Blackie Academic and Professional, New York, 1993.

[10] J. Huang, C. Cui, G. Yan, J. Huang, M. Zhang, A study on degradation of composite material PBS/PCL. Polym. Polym. Compos. 24 (2016) 143-148, https://doi.org/10.1177/096739111602400209.

[11] E. Malikmammadov, T.E. Tanir, A. Kiziltay, V. Hasirci, N. Hasirci, PCL and PCL-based materials in biomedical applications. J. Biomater. Sci. Polym. Ed. 29 (2018) 863-893, https://doi.org/10.1080/09205063.2017.1394711.

[12] S.A. Rafiqah, A. Khalina, A.S. Harmaen, I.A. Tawakkal, K. Zaman, M. Asim, M.N. Nurrazi,

C.H Lee,. A review on properties and application of bio-based poly(butylene succinate). Polymers (2021) 13, 1436, https://doi.org/10.3390/polym13091436.

[13] M.I. Peñas, R.A. Pérez-Camargo, R. Hernández, A.J. Müller, A Review on Current Strategies for the Modulation of Thermomechanical, Barrier, and Biodegradation Properties of Poly (Butylene Succinate)(PBS) and Its Random Copolymers. Polymers 14 (2002) 1025, https://doi.org/10.3390/polym14051025.

[14] O. Platnieks, S. Gaidukovs, V.K. Thakur, A. Barkane, S. Beluns, Bio-based poly (butylene succinate): Recent progress, challenges and future opportunities. Euro. Polym. J. 161 (2021) 110855, https://doi.org/10.1016/j.eurpolymj.2021.110855.

[15] R. Muthuraj, M. Misra, A.K. Mohanty, Biodegradable compatibilized polymer blends for packaging applications: A literature review. J. App. Polym. Sci. 135 (2018) 45726, https://doi.org/10.1002/app.45726.

[16] R.M. Mohamed, K. Yusoh, A review on the recent research of polycaprolactone (PCL). Adv. Mat. Res. 1134 (2016) 249-255, https://doi.org/10.4028/www.scientific.net/AMR.1134.249.

[17] T.P. Gumede, A.S. Luyt, A.J. Müller, Review on PCL, PBS, and PCL/PBS blends containing carbon nanotubes, Express Polym. Lett. 12 (2018) 505–529, http://hdl.handle.net/10576/6808.

[18] P. Nugroho, H. Mitomo, F. Yoshii, T. Kume, K. Nishimura, Improvement of processability of PCL and PBS blend by irradiation and its biodegradability. Macromol. Mater. Eng. 286 (2001) 316-323, https://doi.org/10.1002/1439-2054(20010501)286:5<316::AID-MAME316>3.0.CO;2-N.

[19] S.E. Fenni, J. Wang, N. Haddaoui, B.D. Favis, A.J. Müller, D. Cavallo, Crystallization and self-nucleation of PLA, PBS and PCL in their immiscible binary and ternary blends. Thermochim. Acta 677 (2019) 117-130, https://doi.org/10.1016/j.tca.2019.03.015.

[20] H.S. Cho, H.S. Moon, M. Kim, K. Nam, J.Y. Kim, Biodegradability and biodegradation rate of poly (caprolactone)-starch blend and poly (butylene succinate) biodegradable polymer under aerobic and anaerobic environment. J. Waste Manag. 31 (2011) 475-480, https://doi.org/ 10.1016/j.wasman.2010.10.029.

[21] S. Ravati, B.D. Favis, Interfacial coarsening of ternary polymer blends with partial and complete wetting structures. Polymer 54 (2013) 6739-6751, https://doi.org/10.1016/j.polymer.2013.10.009.

[22] M. M. Reddy, A. K. M. MohantyMisra, Biodegradable blends from plasticized soy meal, polycaprolactone,and poly(butylene succinate). Macromol. Mater. Eng. 297(2012) 455–463, https://doi.org/10.1002/mame.201100203.

[23] E. Can, S. Bucak, E. Kinaci, A. C. Çalikoğlu, G. T. Köse, Polybutylene succinate (PBS) - polycaprolactone (PCL) blends compatibilized with poly(ethylene oxide)-blockpoly(propylene oxide)-block-poly(ethylene oxide) (PEOPPO-PEO) copolymer for biomaterial applications. Polym. Plast. Technol. Eng. 53 (2014) 1178–1193, https://doi.org/10.1080/03602559.2014.886119.

[24] Z. Qiu, M. Komura, T. Ikehara, T. Nishi, Miscibility and crystallization behavior of biodegradable blends of two aliphatic polyesters. Poly (butylene succinate) and poly (ε-caprolactone). Polymer 44 (2003) 7749-7756, https://doi.org/10.1016/j.polymer.2003.10.013.

[25] A. Sadeghi, S. M. Mousavi, E. Saljoughi, S. Kiani, Biodegradable membrane based on polycaprolactone/polybutylene succinate: Characterization and performance evaluation in wastewater treatment. J. App. Polym. Sci. 138 (2021) 50332, https://doi.org/10.1002/app.50332.

[26] W. Hong, J. H. Chang, I. C. Y. Chang, Y. S Sun,. Phase behavior in thin films of weakly segregated block copolymer/homopolymer blends. Soft Matter 17 (2021) 9189-9197, https://doi.org/10.1039/D1SM01005K.

[27] Y.H. Lin, C. C. Shiu, T.L. Chen, H.L. Chen, J.C. Tsai, Solubilization behavior of homopolymer in its blend with the block copolymer displaying the feature of lower critical ordering transition. Polymers 13 (2021) 3415, https://doi.org/10.3390/polym13193415.

[28] H. Mei, J. P. Mahalik, D. Lee, T.S. Laws, T. Terlier, G.E. Stein, R. Kumar, R. Verduzco, Understanding interfacial segregation in polymer blend films with random and mixed side chain bottlebrush copolymer additives. Soft Matter 17 (2021) 9028-9039, https://doi.org/10.1039/D1SM01146D.

[29] K. Samadi, M. Francisco, S. Hegde, C.A. Diaz, T.A. Trabold, E.M. Dell, C.L. Lewis, Mechanical, rheological and anaerobic biodegradation behavior of a Poly (lactic acid) blend containing a Poly (lactic acid)-co-poly (glycolic acid) copolymer. Polym. Degrad. Stab. 170 (2019) 109018, https://doi.org/10.1016/j.polymdegradstab.2019.109018.

[30] M.V. Candal, I. Calafel, N. Aranburu, M. Fernández, G. Gerrica-Echevarria, A. Santamaria, A.J. Müller, Thermo-rheological effects on successful 3D printing of biodegradable polyesters. Addit. Manuf. 36 (2020) 101408, https://doi.org/10.1016/j.addma.2020.101408.

[31] Data available online: https://uk.ravagochemicals.com/capa-6250/

[32] M. Safari, I. Otaegi, N. Aramburu, G. Guerrica-Echevarria, A. M. M. de Ilarduya, H. Sardon, A.J. Müller, Synthesis, Structure, Crystallization and Mechanical Properties of Isodimorphic PBS-ran-PCL Copolyesters. Polymers 13 (2021) 2263, https://doi.org/10.3390/polym13142263.

[33] A.T. Lorenzo, M.L. Arnal, J. Albuerne, A.J. Müller, DSC isothermal polymer crystallization kinetics measurements and the use of the Avrami equation to fit the data: Guidelines to avoid common problems. Polym. Test. 26 (2007) 222-231, https://doi.org/10.1016/j.polymertesting.2006.10.005.

[34] R.A. Pérez-Camargo, G.M. Liu, D.J. Wang, A.J. Müller, Experimental and data fitting guidelines for the determination of polymer crystallization kinetics. Chin. J. Polym. Sci. (2022), https://doi.org/10.1007/s10118-022-2724-2.

[35] J.D. Hoffman, J.J. Weeks, Melting process and equilibrium melting temperature of polychlorotrifluoroethylene, J. Res. Natl. Bur. Stand. (1962) 13-28, https://doi.org/10.1.1.465.6222.

[36] H. Marand, S.J. Xu, Srinivas, Determination of the equilibrium melting temperature of polymer crystals: linear and nonlinear Hoffman− Weeks extrapolations. Macromolecules 31 (1998) 8219-8229, https://doi.org/10.1021/ma980747y.

[37] M.I. Peñas, C. Ocando, E. Penott-Chang, M. Safari, T.A. Ezquerra, E. Rebollar, A. Nogalesd, R. Hernández, A.J. Müller, Nanostructural organization of thin films prepared by sequential dip-coating deposition of poly (butylene succinate), poly (ε-caprolactone) and their copolyesters (PBS-*ran*-PCL). Polymer 226 (2021) 123812.38, https://doi.org/10.1016/j.polymer.2021.123812.

[38] D.W. Van Krevelen, Properties of Polymers, fourth ed., Elsevier Science 2009, 109-127, ISBN: 9780080548197.

[39] P. Rahul, K. Mezghani, P.J. Phillips, Crystallization kinetics of polymers. Physical properties of polymers handbook. Springer, New York, NY, 2007. 625-640.

[40] I. Arandia, A. Mugica, M. Zubitur, A. Arbe, G. Liu, D. Wang, R. Mincheva, P. Dubois, A. J. Müller, How composition determines the properties of isodimorphic poly (butylene succinate-ran-butylene azelate) random biobased copolymers: from single to double crystalline random copolymers. Macromolecules 48 (2015) 43-57, https://doi.org/10.1021/ma5023567.

[41] V. Arrighi, J.M. Cowie, S. Fuhrmann, A. Youssef, Miscibility criterion in polymer blends and its determination. Encyclopedia of polymer blends (2010) 153-198, https://doi.org/10.1002/9783527805204.ch5.

[42] D. Herrera, J.C. Zamora, A. Bello, M. Grimau, E. Laredo, A.J. Müller, T.P. Lodge, Miscibility and crystallization in polycarbonate/poly (ε-caprolactone) blends: Application of the self-concentration model. Macromolecules (2005) 38(12), 5109-5117, https://doi.org/10.1021/ma050481c.

[43] T.P. Lodge, T.C. McLeish, Self-concentrations and effective glass transition temperatures in polymer blends. Macromolecules (2000), 33(14), 5278-5284. https://doi.org/10.1021/ma9921706.

[44] C.C. Huang, M.X. Du, B.Q. Zhang, C.Y. Liu, Glass Transition Temperatures of Copolymers: Molecular Origins of Deviation from the Linear Relation. Macromolecules 55 (2022) 8, 3189–3200, https://doi.org/10.1021/acs.macromol.1c02287.

[45] W. Tu, Y. Wang, X. Li, P. Zhang, Y. Tian, S. Jin, L. M. Wang, Unveiling the Dependence of Glass Transitions on Mixing Thermodynamics in Miscible Systems. Sci. Rep. 5 (2015) 1-5, https://doi.org/10.1038/srep08500.

[46] M. Safari, A. Martinez de Ilarduya, A. Mugica, M. Zubitur, S. Muñoz-Guerra, A.J. Müller, Tuning the thermal properties and morphology of isodimorphic poly [(butylene succinate)-*ran*-(ε-caprolactone)] copolyesters by changing composition, molecular weight, and thermal history. Macromolecules 51 (2018) 9589-9601, https://doi.org/10.1021/acs.macromol.8b01742.

[47] C. Ciulik, M. Safari, A.M. de Ilarduya, J.C. Morales-Huerta, A. Iturrospe, A. Arbe, A.J. Müller, S. Muñoz-Guerra, Poly (butylene succinate-ran-ε-caprolactone) copolyesters: Enzymatic synthesis and crystalline isodimorphic character. Eur. Polym. J. 95 (2017) 795-808, https://doi.org/10.1016/j.eurpolymj.2017.05.002.

[48] M. Safari, A. Mugica, M. Zubitur, A. Martinez de Ilarduya, S. Muñoz-Guerra, A.J. Müller, Controlling the isothermal crystallization of isodimorphic PBS-*ran*-PCL random copolymers by varying composition and supercooling. Polymers 12 (2019) 17, https://doi.org/10.3390/polym12010017.

[49] M. Safari, L. Leon Boigues, G. Shi, J. Maiz, G. Liu, D. Wang, A.J. Müller, Effect of Nanoconfinement on the Isodimorphic Crystallization of Poly (butylene succinate-ran-caprolactone) Random Copolymers. Macromolecules 53 (2020) 6486-6497, https://doi.org/10.1021/acs.macromol.0c01081.

[50] D.G. Papageorgiou, E. Zhuravlev, G.Z. Papageorgiou, D. Bikiaris, K. Chrissafis, C. Schick, Kinetics of nucleation and crystallization in poly (butylene succinate) nanocomposites. Polymer 55 (2014) 6725-6734, https://doi.org/10.1016/j.polymer.2014.11.014.

[51] G. Liu, L. Zheng, X. Zhang, C. Li, S. Jiang, D. Wang, Reversible Lamellar Thickening Induced by Crystal Transition in Poly(butylene succinate). Macromolecules (2012), 45(13): 5487-5493, https://doi.org/10.1021/ma300530a.

[52] R.A. Pérez-Camargo, G. Liu, D. Cavallo, D. Wang, A.J. Müller, Effect of the Crystallization Conditions on the Exclusion/Inclusion Balance in Biodegradable Poly (butylene succinate-ran-butylene adipate) Copolymers. Biomacromolecules 21 (2020) 3420-3435, https://doi.org/10.1021/acs.biomac.0c00847.

[53] S.E. Fenni, D. Cavallo, A.J. Müller, Nucleation and crystallization in bio-based immiscible polyester blends. Therm. Prop. Bio-based Polym. (2019) 219-256, https://doi.org/10.1007/12-2019-48.

[54] R.A. Pérez-Camargo, B. Fernández-d'Arlas, D. Cavallo, T. Debuissy, E. Pollet, L. Avérous, A.J. Müller, Tailoring the structure, morphology, and crystallization of isodimorphic poly (butylene succinate-ran-butylene adipate) random copolymers by changing composition and

thermal   history.   Macromolecules   50   (2017)   597-608, https://doi.org/10.1021/acs.macromol.6b02457.

[55] Y. He, B. Zhu, Y. Inoue, Hydrogen bonds in polymer blends. Prog. Polym. Sci. 29 (2004) 1021-1051, https://doi.org/10.1016/j.progpolymsci.2004.07.002.

[56] J.D. Hoffman, G.T. Davis, J. I. Lauritzen, The rate of crystallization of linear polymers with chain folding. In Treatise on Solid State Chemistry; Springer: Washington, DC, USA, 1976, 497–614.

[57] M. Avrami, Granulation, Phase Change, and Microstructure Kinetics of Phase Change. III J. Chem. Phys. 9 (1941) 177– 184, https://doi.org/10.1063/1.1750872.

[58] T. Nishi, T.T. Wang, Melting point depression and kinetic effects of cooling on crystallization in poly (vinylidene fluoride)-poly (methyl methacrylate) mixtures. Macromolecules 8 (1975) 909-915, https://doi.org/10.1021/ma60048a040.

[59] Z. Qiu, T. Ikehara, T. Nishi, Miscibility and crystallization in crystalline/crystalline blends of poly (butylene succinate)/poly (ethylene oxide). Polymer 44 (2003) 2799-2806, https://doi.org/10.1016/S0032-3861(03)00149-6.

[60] H.B. Eitouni, N.P. Balsara, Thermodynamics of polymer blends. Physical Properties of Polymers Handbook. Springer, New York, NY, 2007, 339-356.

[61] H. Hu, L.D. Douglas, Crystal structure of poly (iε-caprolactone). Macromolecules (1990) 23.21, 4604-4607, https://doi.org/10.1021/ma00223a017.

[62] H. Bittiger, R.H. Marchessault, W.D. Niegisch, Crystal structure of poly-ε-caprolactone. Acta. Crys. 26 (1970) 1923-1927, https://doi.org/10.1107/S0567740870005198.

[63] X. Wang, J. Zhou, L. Li, Multiple melting behavior of poly (butylene succinate). Eur. Polym. J. 43 (2007) 3163-3170, https://doi.org/10.1016/j.eurpolymj.2007.05.013.

[64] Y. Ichikawa, J. Suzuki, J. Washiyama, Y. Moteki, K. Notguchi, K. Okuyama, Strain-induced crystal modification in poly(tetramethylene succinate). Polymer 35 (1994) 3338–3339, https://doi.org/10.1016/0032-3861(94)90144-9.

[65] R.A. Pérez-Camargo, I. Arandia, M. Safari, D. Cavallo, N. Lotti, M. Soccio, A.J. Müller, Crystallization of isodimorphic aliphatic random copolyesters: Pseudo-eutectic behavior and double-crystalline materials. Eur. Polym. J. 101 (2018) 233-247, https://doi.org/10.1016/j.eurpolymj.2018.02.037.